

The 11th Annual SLRI User Meeting 2023

The Book of Abstract AUM2023

THE 11TH ANNUAL SLRI USER MEETING 2023: AUM2023

21th July 2023

The sukosol Hotel, Bangkok



User Service Section

Synchrotron Light Research Institute (Public Organization)

userservice@slri.or.th



www.slri.or.th



THAI
SYNCHROTRON
NATIONAL LAB

List of Abstracts

| | |
|--|----|
| Applicability of Silicon K-edge X-ray Absorption Spectroscopy in Soil Systems _____ | 1 |
| BiOBr-based heterojunction for the photo-enhanced rechargeable zinc-air batteries _____ | 2 |
| Biomaterials Bacterial Cellulose Compositing with MgAl-LDH Nanosheet for Utilizing as the Triboelectric Nanogenerator _____ | 3 |
| CATALYTIC CO ₂ HYDROGENATION TO AROMATIC HYDROCARBONS OVER Fe _x O _y /ZSM-5 ZEOLITE CATALYST UNDER MAGNETIC FIELD _____ | 4 |
| Catalytic LPG conversion over Fe-Ga modified ZSM-5 zeolite catalysts with different particle sizes: Effect of confined-space zeolite and external magnetic field _____ | 5 |
| Catalytic testing of glucose conversion to 5-HMF in biphasic solution over supported Fe-catalysts _____ | 6 |
| Cause of color on amethyst samples under an <i>In-situ</i> heating condition _____ | 7 |
| Charge Storage Properties of Lithium-Based “Water-in-Salt” Electrolytes and Its Electrochemistry _____ | 8 |
| Chitosan-based Biomaterials Enhanced Performance with Organic Piezoelectric Glycine for Hybrid Piezo-Triboelectric Nanogenerator _____ | 9 |
| Cotton-based Triboelectric Nanogenerator with Enhancing Output Efficiency with Inorganic Dyes _____ | 10 |
| Crystallographic and Spectroscopic Investigations on Oxidative Coordination in the Heteroleptic Mononuclear Complex of Cerium and Benzoxazine Dimer _____ | 11 |
| Effect of Copper Phyllosilicate Catalyst for Selective Hydrogenation of Fatty Acid Methyl Esters (FAMES) to Fatty Alcohol _____ | 12 |
| Effect of reduction efficiency on CO ₂ methanation of supported nickel catalysts using in situ/operando XAS investigation _____ | 13 |
| Effect of Sm ³⁺ doping of magnetic and electrical properties of ternary cobaltite spinels _____ | 14 |
| Energetic and reversible “layered to layered” transformation of manganese dioxide in wet nonaqueous zinc-ion battery based on dimethyl sulfoxide electrolyte _____ | 15 |
| Eu ₂ O ₃ doped silicoborate glasses for scintillation material application: Luminescence ability and X-ray imaging _____ | 16 |
| Eu ³⁺ Doped Na ₂ O- Gd ₂ O ₃ -BaO - B ₂ O ₃ -P ₂ O ₅ Glasses for X-ray Scintillator Applications _____ | 17 |
| Flexible Hybrid Thermoelectric-Triboelectric Nanogenerator Based on Cotton Fabric and Polyaniline/Carbon Nanotube (PANI/CNT) Composite _____ | 18 |
| FLEXIBLE SENSOR BASED ON BACTERIAL CELLULOSE – TITANIUM DIOXIDE NANOTUBES COMPOSITE _____ | 19 |
| High-resolution X-ray Imaging and Pulse Height Spectra of CeF ₃ -doped Fluorophosphate Glasses for Scintillator Applications _____ | 20 |

| | |
|---|----|
| Homogenous Zn deposition by fly ash-cellulose separator for high-performance Zn ²⁺ batteries _____ | 21 |
| In Situ X-Ray Absorption Spectroscopy Investigation of Synergistic Effect on Mn-Fe Active Sites in OER and ORR _____ | 22 |
| Investigation of CO ₂ hydrogenation on CuFe ₂ O ₄ /SBA-15 catalysts via in-situ/operando XAS _____ | 23 |
| Metal-carbon electrocatalysts for oxygen-involving reactions _____ | 25 |
| Multi-phase TiO ₂ Doped with Ag as a Sensing Material for Nitrite Detection _____ | 26 |
| Organic-based Three-Phase Composites for Flexible Hybrid Piezoelectric-Triboelectric Nanogenerator ____ | 27 |
| Oxidation State of Fe in Volcanic Rocks of Thailand as Potential Raw Materials for Mars Regolith Simulant _ | 28 |
| Physical and Photoluminescence Investigation of Eu ³⁺ Doped Gadolinium Borate Scintillating Glass _____ | 29 |
| Platinum and PtNi nanoparticle-supported multiwalled carbon nanotube electrocatalysts prepared by one-pot pyrolytic synthesis with an ionic liquid for dye-sensitized solar cells _____ | 31 |
| Rayon Fabric-P3HT composite for High Efficient Triboelectric-Thermoelectric Nanogenerator _____ | 32 |
| Relationship of crystallization behavior by In-situ synchrotron wide-angle X-ray scattering and resistant starch formation of debranched cassava starches _____ | 33 |
| Remineralizing effect of nanohydroxyapatite-containing varnish on artificial enamel lesion _____ | 34 |
| Selective acetylene removal from ethylene-rich feed by cross-metathesis over supported WO ₃ catalysts ____ | 35 |
| Solar-light-driven photocatalytic degradation of organic pollutants in wastewater by using heterojunction photocatalyst _____ | 36 |
| Stable and Efficient Dopant-free P3HT-based Perovskite Solar Cell for Indoor Application via Organometallic Interlayer _____ | 37 |
| Structural characterization and XANES spectra of aluminium potassium gadolinium phosphate glasses doped with Er ₂ O ₃ _____ | 39 |
| Structural correlation to optical properties of Er ³⁺ ion doped alkali boro-phosphate glasses using synchrotron technique _____ | 40 |
| Synchrotron Radiation Science in Industrial Materials _____ | 41 |
| Synchrotron studies of Ag ⁺ and Dy ³⁺ ions in zinc lanthanum aluminum borate glasses synthesized using Novel Microwave melt-quenching technique _____ | 42 |
| Synthesis and characterization of Gd ₂ MoB ₂ O ₉ : CeF ₃ phosphors doped ZnO: BaO: B ₂ O ₃ glasses by microwave sintering for scintillation materials _____ | 43 |
| The investigation of Cu species transformation during the reduction of K ⁺ doped copper phyllosilicate by the <i>in-situ</i> TR-XANES _____ | 45 |
| Tuning Surface Energy to Enhance MoS ₂ Nanosheets Production via Liquid Phase Exfoliation: Understanding of Electrochemical Adsorption of Cesium Chloride _____ | 46 |

| | |
|--|----|
| Utilizing Synchrotron Radiation for Characterizations of the p-Cu ₂ O and n-g-C ₃ N ₄ Semiconductors for Tribovoltaic Nanogenerator Development | 47 |
| UV-C sensors based on beta gallium oxide | 48 |
| Woven Fabric-based Triboelectric Nanogenerators: Effect of Weaving pattern and Multilayer Structure Design on the Electrical Output | 49 |

Applicability of Silicon K-edge X-ray Absorption Spectroscopy in Soil Systems

A. Saentho^{1, 2, 3}, C. Sjöstedt⁴, N. Prakongkep⁵, W. Klysubun⁶,
J.P. Gustafsson⁴, and W. Wisawapipat^{1, 2, 3,*}

¹ Department of Soil Science, Faculty of Agriculture, Kasetsart University, Bangkok 10900, Thailand

² Center for Advanced Studies for Agriculture and Food, KU Institute for Advanced Studies, Kasetsart University, Bangkok 10900, Thailand

³ Center for Advanced Studies in Nanotechnology for Chemical, Food and Agricultural Industries, KU Institute for Advanced Studies, Kasetsart University, Bangkok 10900, Thailand

⁴ Department of Soil and Environment, Swedish University of Agricultural Sciences, Box 7014, Uppsala 750 07, Sweden

⁵ Office of Science for Land Development, Land Development Department, Bangkok 10900, Thailand

⁶ Synchrotron Light Research Institute, Muang District, Nakhon Ratchasima 30000, Thailand
*Email: worachart.w@ku.th

ABSTRACT

Silicon (Si) is an abundant element in terrestrial systems and makes key contributions to agriculture, environments, and industries; however, current knowledge of Si speciation and surface complexes in soil systems is limited. Herein, we examined Si speciation in tropical soil clays using X-ray absorption near edge structure (XANES) spectroscopy and identified surface complexes of Si adsorbed to iron oxyhydroxides, major sorbents, using extended X-ray absorption fine structure (EXAFS) spectroscopy. The XANES data revealed dominances of pre-white-line feature, white-line position and intensity, and post-edge numbers and positions of Si reference spectra, which were applicable to differentiating Si reference standard spectra and identifying the tropical soil clays. The EXAFS data showed that the bidentate mononuclear (²E) edge-sharing complex was the main molecular configuration of the Si tetrahedra on the Fe oxyhydroxide surfaces, irrespective of pH, Si surface loadings, and Fe crystallinity. However, the EXAFS fittings showed a high amplitude reduction factor, indicating possible uncertainties of the fittings, which required further studies.

BiOBr-based heterojunction for the photo-enhanced rechargeable zinc-air batteries

Amornrat khampuanbut¹, Soorathep Kheawhom^{2,3}, Wathanyu Kao-ian²,
Wanwisa Limphirat⁵, and Prasit Pattananuwat^{1,3,4*}

¹*Departments of Materials Science, Faculty of Science, Chulalongkorn University, Bangkok, 10330, Thailand*

²*Departments of Chemical Engineering, Faculty of Engineering, Chulalongkorn university, Bangkok, 10330, Thailand*

³*Center of Excellence on Advanced Materials for Energy Storage, Chulalongkorn University, Bangkok 10330, Thailand*

⁴*Center of Excellence on Petrochemical and Materials Technology, Chulalongkorn University, Bangkok 10330, Thailand*

⁵*Synchrotron Light Research Institute, 111 University Avenue, Suranaree, Muang, Nakhon Ratchasima 30000 Thailand*

**Email: Prasit.pat@chula.ac.th*

ABSTRACT

The suitable energy level of the synergistic composite materials is the key factor for photocatalytic properties of the oxygen reduction reaction (ORR) and the oxygen evolution reaction (OER) [1-3]. Here, the g-C₃N₄/BiOBr heterojunction was successfully synthesized by hydrothermal process and used as a bifunctional cathode for photo-enhanced rechargeable zinc-air batteries. Under LED condition, the ORR and OER performance of g-C₃N₄/BiOBr at 0.4 V vs RHE and 1.9 V vs RHE were ca. 52.43% and ca. 61.90%, respectively, in comparison with the absence of LED. The g-C₃N₄/BiOBr heterojunction possesses an approximately 4e⁻ reactions pathway, suggesting the better activity of ORR and OER and the favorable reaction for zinc-air batteries. In addition, under LED condition can decrease the potential gap (0.06 V), leading to an increase in round-trip efficiency (RTE) of 2.71%. Furthermore, in-situ X-ray absorption spectroscopy (in situ-XAS) technique was used to understand the charge/discharge processes of photo-enhance rechargeable zinc-air battery. In conclusion, the g-C₃N₄/BiOBr heterojunction demonstrates the positive role of visible-light-driven photo-enhanced rechargeable zinc-air batteries.

REFERENCES

1. C. Tomon, S. Sarawutanukul, S. Duangdangchote, A. Krittayavathananon, and M. Sawangphruk, Photoactive Zn-air batteries using spinel-type cobalt oxide as a bifunctional photocatalyst at the air cathode, *Chem, Comm.*, 55, 5855, 2019.
2. X. Liu, Y. Yuan, J. Liu, B. Liu, X. Chen, j. Ding, X. Han, Y. Deng, C. Zhong, and W. Hu, Utilizing solar energy to improve the oxygen evolution reaction kinetics in zinc-air battery, *Nat. Commun.*, 10, 4746, 2019.
3. R. Ren, G. Liu, J. Y. Kim, R. E. A. Ardhi, M. X. Tran, W. Yang, and J. K. Lee, Photoactive g-C₃N₄/CuZIF-67 bifunctional electrocatalyst with staggered p-n heterojunction for rechargeable Zn-air batteries, *Appl. Catal. B*, 306, 121096, 2022.

Biomaterials Bacterial Cellulose Compositated with MgAl-LDH Nanosheet for Utilizing as the Triboelectric Nanogenerator

N. Suktep¹, S. Pongampai², P. Pakawanit³, T. Maluangnont⁴,
N. Vittayakorn⁵ and T. Charoonsuk^{1*}

¹*Department of Materials Science, Faculty of Science, Srinakharinwirot University, Sukhumvit 23, Watthana, Bangkok 10110, Thailand*

²*Department of Physics, Faculty of Science, King Mongkut's University of Technology Thonburi, Bangkok 10140, Thailand*

³*Synchrotron Light Research Institute (Public Organization), 111 University Avenue, Muang District, Nakhon Ratchasima 30000, Thailand*

⁴*College of Materials Innovation and Technology, King Mongkut's Institute of Technology Ladkrabang, Bangkok 10520, Thailand*

⁵*Advanced Materials Research Unit, School of Science, King Mongkut's Institute of Technology Ladkrabang, Bangkok 10520, Thailand*

**Email: thitiratc@g.swu.ac.th*

ABSTRACT

Implantable medical electronics, i.e. cardiac pacemakers (1), are remedial tools for the improvement of the life of patients suffering from cardiovascular diseases. However, a new type of technology is needed to replace the repeated surgery for battery recharging. This work focuses on fabricating the triboelectric nanogenerators (TENG) to be the efficient power supply for those medical devices and sensors. The bacterial cellulose (BC) was selected as the main material. Various content of magnesium aluminum layer double hydroxide nanosheets (MgAl-LDH NSs) is add to improve the electrical output efficiency. The BC/MgAl-LDH composite phase was confirmed. Importantly, according to the crucial role of percolation threshold. The well distributed MgAl-LDH NSs inside the BC matrix is investigated by the Synchrotron X-ray tomographic microscopy (SR-XTM) technique. The SR-XTM provides 3D images insight internal dispersibility, relating to filler content. The present BC/MgAl-LDH NSs TENG within 1.5 wt% provides the maximum output voltage (V_{oc}) and current (I_{sc}) of 91 V and 9.7 μ A, which is 3 times higher than pristine BC. The successful fabrication of BC-based TENG can confirm the possibility of using biomaterials as the main materials for TENG and will be beneficial for developing self-powered pacemakers or other medical devices.

REFERENCES

1. H. Ouyang and F. Xie, *Nature Communications* **10**, 1821 (2019).

CATALYTIC CO₂ HYDROGENATION TO AROMATIC HYDROCARBONS OVER Fe_xO_y/ZSM-5 ZEOLITE CATALYST UNDER MAGNETIC FIELD

R. Chotchaipitakkul¹ and M. Chareonpanich^{1,2,*}

¹ KU-Green Catalysts Group, Department of Chemical Engineering, Faculty of Engineering, Kasetsart University, Bangkok 10900, Thailand

² Center for Advanced Studies in Nanotechnology for Chemical, Food and Agricultural Industries, Kasetsart University, Bangkok 10900, Thailand

Email: fengmtc@ku.ac.th

ABSTRACT

Based on the green and circular economy, an external magnetic field is applied with an attempt to enhance the catalytic activity and selectivity to produce value-added chemicals and feedstock from CO₂ hydrogenation reaction. In this work, a confined-space ZSM-5 zeolite with molecular sieve property, in conjunction with an external magnetic field was employed to manipulate the iron oxide phase transformation over the Fe_xO_y/ZSM-5 catalysts, and consequently intensify the CO₂ conversion and selective aromatic hydrocarbon production. The in-situ X-ray absorption near-edge structure (XANES) technique is applied to verify the iron oxide phase transformation. The iron oxide phases were observed under various reduction times in combination with different magnetic flux intensities. Subsequently, the resulting catalysts were employed for CO₂ hydrogenation under magnetic field. The Fe_xO_y/ZSM-5 catalyst with a reduction time of 3.0 h and magnetic flux intensity of 20.7 mT, containing a predominant phase of Fe₃O₄, exhibited the highest CO₂ conversion, which was 1.4–1.7 times greater than that observed in the absence of magnetic field. Moreover, the selectivity of monocyclic aromatics was increased by 9.0 times compared to those without magnetic field. The improvements of catalytic activity and selectivity towards aromatic hydrocarbons could be attributed to the synergistic promotion between the confined-space ZSM-5 zeolite and external magnetic field. Not only the rearrangement of iron oxide species along with the alignment of magnetic field direction are induced, but the diffusion of reactant gases is also controlled. These phenomena facilitate the formation of Fe₃O₄ and FeO phases. Thus, olefins are formed through reverse water-gas shift reaction and consecutive chain growth reaction via Fischer-Tropsch synthesis, which further undergo aromatization reaction to produce aromatics within the confined-space ZSM-5 zeolite. This reaction system, therefore, has potential application in a variety of catalytic reactions by enhancing specific gas adsorption and gas-solid interactions in green and sustainable ways.

Catalytic LPG conversion over Fe-Ga modified ZSM-5 zeolite catalysts with different particle sizes: Effect of confined-space zeolite and external magnetic field

Zehui Du^{1,2} and Metta Chareonpanich^{1,2,*}

¹ KU-Green Catalysts Group, Department of Chemical Engineering, Faculty of Engineering, Kasetsart University, Bangkok 10900, Thailand

² Center for Advanced Studies in Nanotechnology for Chemical, Food and Agricultural Industries, Kasetsart University, Bangkok 10900, Thailand

Email: fengmtc@ku.ac.th

ABSTRACT

In this work, the concepts of green and efficient utilization have been applied in order for moving towards carbon neutrality. Accordingly, the confined-space molecular-sieve properties of ZSM-5 zeolite were applied in cooperation with an external magnetic field with the aim to improve the catalytic LPG conversion and the selectivity of BTX (benzene, toluene, and xylenes) over Fe-Ga/ZSM-5 zeolites (0.5 wt.% Ga and 0.1 wt.% Fe). Effect of ZSM-5 particle sizes (0.6 μm , 1.1 μm , and 22.1 μm) on BTX yields and toluene to monoaromatic hydrocarbons were examined under magnetic field at a flux intensity of 28.7 mT in North-to-South direction and compared to those without magnetic field. The highest LPG conversion over the Fe-Ga/ZSM-5 catalyst was observed when using ZSM-5 particles with a size of 1.1 μm under an external magnetic field. This conversion rate was found to be 1.2 times greater than that achieved without a magnetic field. The BTX yield was also increased by factors of 1.5 compared to those without magnetic field. The outstanding performance can be attributed to the synergistic effects between the external magnetic field and limited mass transfer within the confined-space zeolite. This combination facilitates and enhances the mass transfer ability and reaction performance of the reactant molecules, leading to the development of green and sustainable innovations for future chemical and separation processes.

Catalytic testing of glucose conversion to 5-HMF in biphasic solution over supported Fe-catalysts

T. Nanmong¹, W. Obrom¹, W. Yingyuen¹, K. Deekamwong²,
P. Tawachkultanadilok², J. Wittayakun², S. Prayoonpokarach²,
Y. Poo-arporn³, S. Loiha^{1*}

¹*Materials Chemistry Research Center, Department of Chemistry, Faculty of Science, Khon Kaen University, Khon Kaen, Thailand*

²*School of Chemistry, Institute of Science, Suranaree University of Technology, Nakhon Ratchasima, Thailand*

³*Synchrotron Light Research Institute, 111 University Avenue, Muang District, Nakhon Ratchasima, 30000 Thailand*
Email: Tatchapol.n@kkumail.com

ABSTRACT

Catalytic conversion of glucose to 5-hydroxymethylfurfural (5-HMF) and levulinic acid is a value-added biomass process. The catalytic reaction is processed via isomerization and dehydration of glucose. Thus, co-catalysts of iron oxide and zeolites with varying Lewis and Brønsted acids were used in this work. 6% w/w of Fe on Fe/MOR and Fe/ZSM-5 catalysts were prepared by the impregnation method. The catalyst structures were characterized by X-ray absorption spectroscopy (XAS) including XRD, FT-IR, TGA, and SEM. The conversion of glucose in both mono- and bi-phasic systems was conducted in a batch reactor setup with different conditions, and products were monitored by HPLC. The findings of this research provide compelling evidence regarding the substantial influence of solvent systems on the conversion of glucose to HMF. Specifically, in the bi-phasic ethanol-water solvent system, the Fe/HMOR catalyst demonstrated a maximum HMF yield of 47.39%. Conversely, Fe/HZSM-5 achieved the highest glucose conversion of 100% and exhibited a considerably maximum HMF yield at the temperature of 200°C. These results indicate the roles of the solvent system, reaction temperature, and catalyst support in glucose conversion to HMF. The bi-phasic system demonstrated superior performance in terms of yield. Moreover, the specific reaction parameters played a crucial role in determining the efficiency and selectivity of the catalyst, emphasizing the need for careful optimization in industrial-scale applications. The findings can guide future research and development efforts toward the efficient synthesis of HMF as a promising renewable platform chemical.

REFERENCES

1. Yan, L., et al., Chapter One - Catalytic valorization of biomass and bioplatfroms to chemicals through deoxygenation, in *Advances in Catalysis*, C. Song, Editor. 2020, Academic Press. p. 1-108..
2. Xin, H., et al., Dehydration of glucose to 5-hydroxymethylfurfural and 5-ethoxymethylfurfural by combining Lewis and Brønsted acid. *RSC Adv.*, 2017. 7: p. 41546-41551.
3. Abdouli, I., et al., Hydrothermal process assisted by photocatalysis: Towards a novel hybrid mechanism driven glucose valorization to levulinic acid, ethylene and hydrogen. *Applied Catalysis B: Environmental*, 2022. 305: p. 121051.

Cause of color on amethyst samples under an *In-situ* heating condition

S. Saengdech¹, W.Wongkokua², C. Saiyasombat³ and N. Monarumit¹

¹Department of Earth Sciences, Faculty of Science, Kasetsart University, Bangkok,
10900 Thailand

²Department of Physics, Faculty of Science, Kasetsart University, Bangkok,
10900 Thailand

³Synchrotron Light Research Institute, Nakhon Ratchasima, 30000 Thailand
Email: sirinapa.sae@ku.th

ABSTRACT

Amethyst is a variety of quartz (SiO₂) showing purple color. The color of amethyst is related to iron (Fe). The purple color of amethyst could turn yellow and colorless after heating at various temperatures. It was previously suggested that the color of amethyst can change due to the change in the Fe oxidation state. However, the cause of the color of amethyst before and after heating related to the Fe oxidation state was still inconclusive. This study aims to identify the Fe oxidation state of amethyst before and after heating and create an energy band model to explain the cause of color in amethyst samples under *In-situ* heating conditions at different temperatures. The spectroscopic techniques used in this study are Energy Dispersive X-Ray Fluorescence Spectrometer, UV-Vis-NIR Spectrophotometer and X-ray Absorption Spectroscopy focused on Fe *K*-edge XANES spectra. As the result, the color of the amethyst has turned yellow and colorless after *in-situ* heating at 500 °C and 700 °C, respectively. There was a change in the UV-Vis-NIR absorption spectra show different peak positions relating to the different energy band gaps. However, Fe *K*-edge XANES spectra on amethyst samples both before and after heating show Fe³⁺ oxidation state. Moreover, the samples show different energy band gaps derived from the Tauc Plot method before and after *In-situ* heating conditions. Therefore, the cause of color on amethyst can be explained by Energy Band Theory with the Fe³⁺ donor states.

Charge Storage Properties of Lithium-Based “Water-in-Salt” Electrolytes and Its Electrochemistry

Aritsa Bunpheng¹, Thanit Saisopa² and Pawin lamprasertkun¹, *

¹*School of Bio-Chemical Engineering and Technology, Sirindhorn International Institute of Technology, Thammasat University, Pathum Thani 12120, Thailand*

²*Department of Applied Physics, Faculty of Sciences and Liberal Arts, Rajamangala University of Technology Isan, Nakhon Ratchasima 30000, Thailand.*

Email: m6522040630@g.sit.tu.ac.th, pawin@sit.tu.ac.th

ABSTRACT

The evaluation of various aqueous-based electrolytes is central to the most in the context of energy storage. The study focuses on comparing traditional "salt-in-water" electrolytes with emerging "water-in-salt" systems, utilizing different lithium salts. The electrolytes investigated include lithium halides, nitrates, sulfates, and lithium bis(trifluoromethanesulfonyl)imide (LiTFSI) in the "water-in-salt" system. The research examines the physical, chemical, and electrochemical properties of each electrolyte, considering their advantages and disadvantages. It also investigates the electrochemical performance and compatibility of the electrolytes with carbon-based materials. To gain a deeper understanding of the interactions between the electrolyte and the electrode's surface, the study employs X-ray Photoelectron Spectroscopy (XPS) technique. XPS analysis provides valuable information about the chemical composition and behavior of the electrolyte at the electrode-electrolyte interface. Overall, this research is to provide with insights into the properties of different electrolytes, enabling them to make informed decisions when selecting suitable electrolytes for energy storage applications.

Chitosan-based Biomaterials Enhanced Performance with Organic Piezoelectric Glycine for Hybrid Piezo-Triboelectric Nanogenerator

S. Ukasi¹, P. Pakawanit², S. Pongampai³, N. Vittayakorn⁴ and
T. Charoonsuk^{1,*},

¹*Department of Materials Science, Faculty of Science, Srinakharinwirot University,
Sukhumvit 23, Watthana, Bangkok 10110, Thailand*

²*Synchrotron Research and Applications Division, Synchrotron Light Research Institute, 111
University Avenue, Muang District, Nakhon Ratchasima, 30000, Thailand*

³*Department of Physics, Faculty of Science, King Mongkut's University of Technology
Thonburi, Bangkok 10140, Thailand*

⁴*Advanced Materials Research Unit, School of Science, King Mongkut's Institute of
Technology Ladkrabang, Bangkok 10520, Thailand*

**Email: thitiratc@g.swu.ac.th*

ABSTRACT

Flexible electronic devices have now tremendous attention, especially in the field of biomedical, baby-care and healthcare applications. One of challenging is to fabricate external power sources for driving those electronic components with excellent output efficiency, flexibility, stretchability and must be able to operate in contact with the human body without irritation and danger [1]. This work fabricated the chitosan (CS) natural biopolymer for piezo-triboelectric nanogenerator (P-TENG) and enhance performance with incorporating the organic piezoelectric gamma glycine (γ -GC). The effect of different loaded γ -GC on the output performance was explored. The 3D visualization of CS/ γ -GC composite films was analysed by Synchrotron Radiation X-ray Tomographic Microscopy (SR-XTM) technique to investigate the distribution of the dispersive particles that important to find the percolation threshold. It was found that the γ -GC was nicely dispersed and not only incorporated on the surface, but was also present in the interior CS matrix. As considering the morphology and dispersibility, a well-connected phase of γ -GC could be seen at the optimum condition 50wt%, percolation threshold that showed the highest electrical output signal. This is due to the morphologically interconnected network structure within the CS polymer enhances charge generation and transformation. The maximum open-circuit (V_{oc}) and short-circuit current (I_{sc}) of ~ 78.81 V and ~ 64 μ A are enhanced. Its maximum output power of ~ 705.96 μ W was achieved, which is ~ 2.8 times higher than that of pristine CS. Additionally, the TENG demonstrated capability of serving as a power supply for small-electronic devices. 2021;12(1):2399.

REFERENCES

1. Petritz A, Karner-Petritz E, Uemura T, Schäffner P, Araki T, Stadlober B, et al. *Nature Communications*, **12**, 2399 (2021).

Cotton-based Triboelectric Nanogenerator with Enhancing Output Efficiency with Inorganic Dyes

S. Navatragulpisit¹, S. Wu¹, P. Ninlaor¹, S. Pongampai², P. Pakawanit³,
N. Vittayakorn⁴, T. Charoonsuk^{1*}

¹Department of Materials Science, Faculty of Science, Srinakharinwirot University,
Sukhumvit 23, Watthana, Bangkok, 10110, Thailand

²Department of Physics, Faculty of Science, King Mongkut's University of Technology
Thonburi, Bangkok 10140, Thailand

³Synchrotron Light Research Institute (Public Organization), 111 University Avenue, Muang
District, Nakhon Ratchasima 30000, Thailand

⁴Advanced Materials Research Unit, School of Science, King Mongkut's Institute of
Technology Ladkrabang, Bangkok 10520, Thailand

*Email: thitiratc@g.swu.ac.th

ABSTRACT

Nowadays, the electronic textiles (E-textiles), which are made from the combination of fabrics and electronic devices, have gained much attention [1] with highly efficient power source is required. This work aims at the development of triboelectric nanogenerator (TENG) to a self-powered for driving electronic components in textile. The TENG is fabricated by using cotton fabric as the main friction material and modified various of functional groups with an inorganic dye. The cotton fabric/CNT composite is used as electrode for excellent flexibility. The 3D visualization of CNT distribution was investigated by using the Synchrotron X-ray Tomographic technique (SR-XTM) to confirm the percolation threshold that is associate to the electricity [2]. As a result, the cotton/reactive blue dyes obviously show the maximum electrical outputs owing to the high electron donor ability from the functional group and metal atom. This condition provides the value at ~ 32.73 V and ~ 36.6 nA for output voltage (V_{OC}) and output current (I_{SC}) with maximum output power (P_{max}) of ~ 243 μ W. That is higher than pure cotton for 2.2 times. It was concluded that the functional groups of each color of dyes show a crucial role for controlling and enhancing the output efficiency. Furthermore, this work also applies the cotton/reactive dyes TENG to be self-power sensor. The authors expect that this research will be useful for the development of energy harvesting devices for utilizing in E-textiles industry in future.

REFERENCES

1. Gonçalves C, Ferreira da Silva A, Gomes J, Simoes R., *Inventions*, **3**, 14 (2018).
2. S Bonardd S, Morales N, Gence L, Saldias C, Angel FA, Kortaberria G, et al., *ACS Applied Materials & Interfaces*, **12**, 13275-13286 (2020).

Crystallographic and Spectroscopic Investigations on Oxidative Coordination in the Heteroleptic Mononuclear Complex of Cerium and Benzoxazine Dimer

W. Wattanathana¹, N. Suetrong¹, P. Kongsamai², K. Chansaenpak³,
N. Chuanopparat⁴, Y. Hanlomyuang¹, P. Kanjanaboos⁵ and
S. Wannapaiboon⁶

¹Department of Materials Engineering, Faculty of Engineering, Kasetsart University, Ladyao, Chatuchak, Bangkok 10900, Thailand

²School of Chemistry, Institute of Science, Suranaree University of Technology, 111 University Avenue, Suranaree, Muang, Nakhon Ratchasima 30000, Thailand

³National Nanotechnology Center, National Science and Technology Development Agency, Thailand Science Park, Khlong Luang 12120, Thailand

⁴Department of Chemistry, Faculty of Science, Kasetsart University, Ladyao, Chatuchak, Bangkok 10900, Thailand

⁵School of Materials Science and Innovation, Faculty of Science, Mahidol University, Nakhon Pathom 73170, Thailand

⁶Synchrotron Light Research Institute, 111 University Avenue, Suranaree, Muang, Nakhon Ratchasima 30000, Thailand
Email :Natapol.sue@ku.th

ABSTRACT

Among lanthanide-based compounds, cerium compounds exhibit a significant role in a variety of research fields due to their distinct tetravalency, high economic feasibility, and high stability of Ce(IV) complexes. Herein, a systematic investigation of crystallographic information, chemical properties, and mechanistic formation of the novel Ce(IV) complex synthesized from cerium(III) nitrate hexahydrate and 2,2'-(methylazanediyl)bis(methylene)bis(4-methylphenol) (MMD) ligand has been explored. According to the analysis of the crystallographic information, the obtained complex crystal consists of the Ce(IV) center coordinated with two nitrate ligands and two bidentate coordinated (N-protonated and O,O-deprotonated) MMD ligands. The fingerprint plots and the Hirshfeld surface analyses suggest that the C–H...O and C–H... π interactions significantly contribute to the crystal packing. The C–H...O and C–H... π contacts link the molecules into infinite molecular chains propagating along the [100] and [010] directions. Synchrotron powder X-ray diffraction (XRD) and X-ray absorption spectroscopy (XAS) techniques have been employed to gain an understanding of the oxidative complexation of Ce(IV)-MMD complex in detail. This finding would provide the possibility to systematically control the synthetic parameters and wisely design the precursor components in order to achieve the desired properties of novel materials for specific applications.

Effect of Copper Phyllosilicate Catalyst for Selective Hydrogenation of Fatty Acid Methyl Esters (FAMES) to Fatty Alcohol

K. Khosukwiat^{1,2}, K. Choojun^{1,2} and T. Sooknoi^{1,2}

¹*Department of Chemistry, School of Science, King Mongkut's Institute of Technology Ladkrabang, Chalongkrung Road, Ladkrabang, Bangkok 10520, Thailand*

²*Catalytic Chemistry Research Unit, School of Science, King Mongkut's Institute of Technology Ladkrabang, Chalongkrung Road, Ladkrabang, Bangkok 10520, Thailand*

ABSTRACT

Hexadecanol or fatty alcohol is one of the most important intermediates to produce many varieties of chemical products, which can be derived from the hydrogenation of methyl palmitate. In this research, the comparative copper phyllosilicate with 20 and 30wt.% Cu loading was synthesized by ammonia hydrothermal method using two different silica colloidal precursors (AS-ammonium stabilized and HS-sodium stabilized) to obtain 20%CuPS-AS, 20%CuPS-HS and 30%CuPS-HS. At 20wt.% Cu loading, 20CuPS-HS showed a slightly higher Cu dispersion (77%, N₂O-TPR) and Cu⁺ species (15%, in situ TR-XANES) than 20CuPS-AS (D_{Cu} 69%, 11% Cu₊ species), presumably due to the presence of Na⁺ as a fluxing agent. Furthermore, the decrease in total acidity of 20CuPS-HS (19 μmol/g) derived from NH₃-TPD was observed, as compared to those of 20CuPS-AS (25 μmol/g). Upon increasing the Cu content from 20 to 30 wt.%, 30CuPS-HS has a lower Cu dispersion due to the higher Cu²⁺_{Sq} species leading to a higher agglomeration. All CuPS catalysts showed a much higher activity for hydrogenation of methyl palmitate (MP) in a continuous fixed-bed reactor at 250 °C under atmospheric H₂, as compared to impregnated 20Cu/SiO₂. Even though 20CuPS-HS showed a slightly lower hydrogenation activity (67%) than 20CuPS-AS (70%) despite the higher Cu dispersion. The significant increase in hexadecanol selectivity was obtained (~3 folds). In fact, the alcohol selectivity of 20CuPS-HS is always higher than those of 20CuPS-AS at all contact times. This could be attributed to the higher Cu⁺ fraction and lower acidity. Though, the increase in Cu content using sodium stabilized silica colloidal precursor led to a decrease in hydrogenation activity due to the lower Cu dispersion. However, the alcohol selectivity of 30CuPS-HS remains high as 20CuPS-HS.

REFERENCES

1. W. Prasanseang, K. Choojun, Y. Poo-arporn, A. Huang, Y. Lin, and T. Sooknoi, *Applied Catalysis A: General* **635**, 118555 (2022).

Effect of reduction efficiency on CO₂ methanation of supported nickel catalysts using in situ/operando XAS investigation

W. Obrom¹ , W. Yingyuen¹ , T. Nanmong¹ , K. Deekamwong² ,
P. Tawachkultanadilok² , J. Wittayakun² , S. Prayoonpokarach² ,
Y. Poo-arporn³ , S. Loiha^{1*}

¹*Materials Chemistry Research Center, Department of Chemistry, Faculty of Science,
Khon Kaen University, Khon Kaen, Thailand*

²*School of Chemistry, Institute of Science, Suranaree University of Technology, Nakhon
Ratchasima, Thailand*

³*Synchrotron Light Research Institute, 111 University Avenue, Muang District, Nakhon
Ratchasima, 30000 Thailand
Email: waranya.ob@kkumail.com*

ABSTRACT

Climate change-related environmental issues including the greenhouse effect and ocean acidification have received a lot of attention. The chemical translation of carbon dioxide (CO₂) into value-added goods might effectively lessen the effects of CO₂ and advance the global carbon cycle. In this study, a series of 5% w/w of Ni supported on silica and zeolites including ZSM-5, A, and ANA catalysts were synthesized. The catalyst structures were characterized by X-ray diffraction analysis (XRD), X-ray absorption spectroscopy (XAS), and Transmission electron microscopes (TEM). The basicity of the catalysts was determined by temperature-programmed desorption (TPD) of carbon dioxide. Catalytic testing of CO₂ -methanation was carried out under in situ/operando XAS. The catalytic conversion of CO₂ increased with increasing temperature up to 400°C. The catalyst supports play an important role in the reaction ability of nickel. Zeolite-type support showed 100% selectivity to methane products. The catalytic conversion percents are ordered as Ni/A > Ni/ZSM-5 > Ni/ANA > Ni/SiO₂, respectively.

REFERENCES

1. Zhang J, Ying Y, Liu J, Xiong B. Mechanistic understanding of CO₂ hydrogenation to methane over Ni/CeO₂ catalyst. *Applied Surface Science*. 2021;558:149866. doi:10.1016/j.apsusc

Effect of Sm³⁺ doping of magnetic and electrical properties of ternary cobaltite spinels

S. Yaemphutchong⁶, W. Deeloed¹, P. Jantaratana², S. Singkammo³,
P. Kanjanaboos⁴, K. Chanseanpak⁵, S. Wannapaiboon³,
W. Wattanathana^{6,*} and Y. Hanlumyuang^{6,*}

¹Department of Chemistry, Faculty of Science, Kasetsart University, Bangkok, 10900 Thailand

²Department of Physics, Faculty of Science, Kasetsart University, Bangkok, 10900 Thailand

³Synchrotron Light Research Institute, 111 University Avenue, Muang District, Nakhon Ratchasima, 30000 Thailand

⁴School of Materials Science and Innovations, Faculty of Science, Mahidol University, Nakhon Pathom, 73170 Thailand

⁵National Nanotechnology Center, National Science and Technology Development Agency, Thailand Science Park, Khlong Luang 12120 Thailand

⁶Department of Materials Engineering, Faculty of Engineering, Kasetsart University, Bangkok, 10900 Thailand
Email: Sila.yae@ku.th

ABSTRACT

NiCo₂O₄ (NCO) and ZnCo₂O₄ (ZCO) are the nickel- and zinc-substituted derivatives of the cobaltite oxide spinel (CoCo₂O₄, CCO), which have been considered as emerging materials in various applications. In this work, NCO, ZCO, and two Sm-doped analogs (Sm-NCO and Sm-ZCO) were synthesized, using oxidative thermal decomposition of their corresponding hydrothermal derived precursors. Phase identification by PXRD confirmed the purity of the spinel phase on all synthesized Sm-doped analogs. The result agrees with XAS result that shown the lack sign of Sm₂O₃ species. Accordingly, it suggested a unique coordination environment of trivalent samarium in the Sm-doped samples. Further investigation revealed porous texture on particle surface and additional specific surface area are caused by the dopant to the analogs. The dopant also hindered an accumulation of nickel and zinc in the precursor, resulting in the deficiency of such elements in the prepared oxides. Consequently, it causes a significant change in magnetics and electrical properties susceptibility by the dilution of nickel- and zinc-substitution effects. The multifunctionality of samarium as presented here provides an example use of lanthanide element to tailor material physical/chemical properties without destroying host crystalline structure.

Energetic and reversible “layered to layered” transformation of manganese dioxide in wet nonaqueous zinc-ion battery based on dimethyl sulfoxide electrolyte

W. Kao-ian¹, J. Sangsawang¹, P. Kidkhunthod², S. Wannapaiboon², M. Suttipong³, P. Pattananuwat^{4,5}, M. T. Nguyen⁶, T. Yonezawa⁶ and S. Kheawhom^{1,5}

¹ Department of Chemical Engineering, Faculty of Engineering, Chulalongkorn University, Bangkok 10330, Thailand

² Synchrotron Light Research Institute, 111 University Avenue, Muang District, Nakhon Ratchasima 30000, Thailand

³ Department of Chemical Technology, Faculty of Science, Chulalongkorn University, Bangkok 10330, Thailand

⁴ Department of Materials Science, Faculty of Science, Chulalongkorn University, Bangkok 10330, Thailand

⁵ Center of Excellence on Advanced Materials for Energy Storage, Chulalongkorn University, Bangkok 10330, Thailand

⁶ Division of Materials Science and Engineering, Faculty of Engineering, Hokkaido University, Hokkaido 060-8628, Japan

ABSTRACT

Due to its excellent reversibility and stability, a dimethyl sulfoxide (DMSO) electrolyte is seen to be a promising nonaqueous electrolyte. Compared to aqueous Zn-MnO₂ systems, ZIBs having DMSO electrolytes, and manganese dioxide (MnO₂) cathodes display inferior rates and capacity performances. However, it is found that the addition of water can improve the performance of DMSO-based ZIBs, even a small amount of water. In this work, the effect of water on the performance of DMSO-based ZIBs is thoroughly investigated. Herein, the layer-type MnO₂ (δ type, birnessite) is used as the main cathode material. Ex-situ/operando X-ray diffraction (XRD) analysis and in-situ X-ray absorption spectroscopy (XAS) results suggest that the existence of water in DMSO electrolytes can lead to changes occurring in the Zn²⁺ intercalated phase. A Zn-birnessite when replaced by a super-hydrated Zn-buserite provides a much improved solid-phase diffusion of Zn²⁺ and surface kinetics. The optimized battery yields the highest capacity of 224 mAh/g and can cycle over 2,500 cycles. This discovery extends the understanding of wet nonaqueous electrolyte chemistry and paves the way towards the practical application of ZIBs.

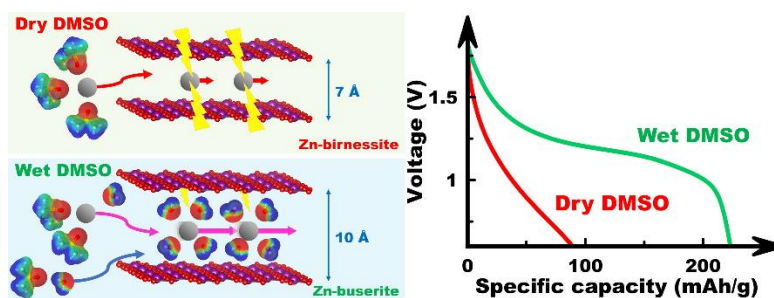


Figure 1. Graphical abstract.

Eu₂O₃ doped silicoborate glasses for scintillation material application: Luminescence ability and X-ray imaging

N. Intachai¹, N. Wantana^{2,3}, S. Kaewjaeng¹, P. Pakawanit⁴, N. Vittayakorn⁵, S. Kothan^{1*}, H.J. Kim⁶, and J. Kaewkhao^{2,3**}

¹Center of Radiation Research and Medical Imaging, Department of Radiologic Technology, Faculty of Associated Medical Sciences, Chiang Mai University, Chiang Mai, 50200, Thailand

²Physics Program, Faculty of Science and Technology, Nakhon Pathom Rajabhat University, Nakhon Pathom, 73000, Thailand

³Center of Excellence in Glass Technology and Materials Science (CEGM), Nakhon Pathom Rajabhat University, Nakhon Pathom, 73000, Thailand

⁴Synchrotron Research and Applications Division, Synchrotron Light Research Institute, 111 University Avenue, Muang District, Nakhon Ratchasima, 30000, Thailand

⁵Advanced Materials Research Unit, School of Science, King Mongkut's Institute of Technology Ladkrabang, Bangkok 10520, Thailand

⁶Department of Physics, Kyungpook National University, Daegu, 41566, South Korea

ABSTRACT

This research aimed to investigate the europium oxide (Eu₂O₃) doped silicoborate glasses for scintillation material application by inspection of physical, optical, luminescence, and x-ray imaging. The glass samples were prepared by changing europium concentrations following component xEu₂O₃ - 40Na₂O - 7.5Gd₂O₃ - 5SiO₂ - (47.5-x)B₂O₃ (x = 0, 1, 2, 3 mol%). The density, molar volume, and other physical parameters have been evaluated as physical properties. The absorption spectra were represented in the length of UV-Vis and NIR region. The photoluminescence and X-ray-induced luminescence spectra showed similar highest intensity at 3 mol% of Eu₂O₃. The Eu³⁺ in the glass matrix produced orange-red luminescence corresponding to the radiative transitions at ⁵D₀ → ⁷F₂. The Chromaticity coordinates of the glasses are placed in a relatively narrow area in the reddish-orange part of the diagram. The emission spectra of 3Eu:7.5Gd glass demonstrated the beneficial effects of Eu₂O₃ addition in glass material, and it can be developed to use as a scintillator material, confirmed by the two-dimension (2D) X-ray image and the three-dimension (3D) reconstruction.

Eu³⁺ Doped Na₂O- Gd₂O₃ -BaO - B₂O₃-P₂O₅ Glasses for X-ray Scintillator Applications

F. Khongchaiyaphum^{1, 2}, S. Kansirin^{1,2}, N. Wantana^{1,2*}, P. Pakawanit⁴,
N. Vittayakorn⁵, N. Chanthima^{1,2}, H.J. Kim³, J. Kaewkhao^{1,2}

*1 Physics Program, Faculty of Science and Technology, Nakhon Pathom Rajabhat
University, Nakhon Pathom, 73000, Thailand*

*2 Center of Excellence in Glass Technology and Materials Science (CEGM), Nakhon
Pathom Rajabhat University, Nakhon Pathom, 73000, Thailand*

*3 Department of Physics, Kyungpook National University, Daegu, 702-701, Republic of
Korea*

*4 Synchrotron Light Research Institute, 111 University Avenue, Muang District, Nakhon
Ratchasima, 30000, Thailand*

*5 Advanced Materials Research Unit, School of Science, King Mongkut's Institute of
Technology Ladkrabang, Bangkok 10520, Thailand*

**Email: wnuanthip@webmail.npru.ac.th*

ABSTRACT

The Na₂O-Gd₂O₃-BaO-B₂O₃-P₂O₅ glasses were doped with varying concentrations of Eu₂O₃ (referred to as Eu:NGBaPB) and prepared using the melt-quenching technique. These glasses were analyzed comprehensively in the physical, optical, chemical groups and photo-/radio- luminescence properties. Furthermore, the X-ray imaging was operated to indicate the practical radiation detection of glass. The addition of Eu₂O₃, the density and refractive index of Eu:NGBaPB glasses increased, while the molar volume decreased. The glass exhibited photon absorption in the UV-NIR regions. Excitation from various sources such as X-ray, ultraviolet, and visible light resulted in a reddish-orange emission at approximately 613 nm, originating from the 5D₀→7F₂ radiation states of Eu³⁺. Energy transfer occurred from Gd³⁺ to Eu³⁺ within the glass. These findings highlight the intriguing potential of the glass for applications as an X-ray scintillator.

REFERENCES

1. I. Khan, G. Rooh, R. Rajaramakrishna, N. Sirsittapokakun, H.J. Kim, J. Kaewkhao, K. Kirdsiri, Energy transfer phenomenon of Gd³⁺ to excited ground state of Eu³⁺ ions in Li₂O-BaO-Gd₂O₃-SiO₂-Eu₂O₃ glasses, Spectrochim. Acta - Part A Mol. Biomol. Spectrosc. 210 (2019) 21–29. <https://doi.org/10.1016/j.saa.2018.11.008>.
2. S. Mao, D.A. Hakeem, S. Su, H. Wen, W. Song, Optical properties of V, Eu doped sodium borosilicate glass, Optik (Stuttg). 229 (2021) 166225. <https://doi.org/10.1016/j.ijleo.2020.166225>.
3. D. Ramachari, L. Rama Moorthy, C.K. Jayasankar, Phonon sideband spectrum and vibrational analysis of Eu³⁺-doped niobium oxyfluorosilicate glass, J. Lumin. 143 (2013) 674–679. [25] S. Singh, S.P. Khatkar, V.B. Taxak, Luminescence and structural properties of Eu³⁺ doped BaY₂ZnO₅ for LED solid-state lighting application, J. Mater. Sci. Mater. Electron. 24 (2013) 4677–4683. <https://doi.org/10.1007/s10854-013-1459-9>.
4. M. Behrendt, S. Mahlik, M. Grinberg, D. Stefańska, P.J. Dereń, Influence of charge transfer state on Eu³⁺ luminescence in LaAlO₃, by high pressure spectroscopy, Opt. Mater. (Amst). 63 (2017) 158–166. <https://doi.org/10.1016/j.optmat.2016.06.052>.
5. N. Wantana, E. Kaewnuam, Y. Tariwong, N.D. Quang, P. Pakawanit, C. Phoovasawat, N. Vittayakorn, S. Kothan, H.J. Kim, J. Kaewkhao, Na₂O-Gd₂O₃-Al₂O₃-P₂O₅ glass scintillator doped with Dy³⁺: X-rays and proton responses, Jpn. J. Appl. Phys. 62 (2023). <https://doi.org/10.35848/1347-4065/ac9876>.

Flexible Hybrid Thermoelectric-Triboelectric Nanogenerator Based on Cotton Fabric and Polyaniline/Carbon Nanotube (PANI/CNT) Composite

P. Mohsom¹, C. Sae-tang¹, C. Khotsombat¹, S. Pongampai², P. Pakawanit³, N. Vittayakorn⁴ and T. Charoonsuk^{1*}

¹Department of Materials Science, Faculty of Science, Srinakharinwirot University, Sukhumvit 23, Watthana, Bangkok 10110, Thailand

²Department of Physics, Faculty of Science, King Mongkut's University of Technology Thonburi, Bangkok 10140, Thailand

³Synchrotron Light Research Institute (Public Organization), 111 University Avenue, Muang District, Nakhon Ratchasima 30000, Thailand

⁴Advanced Materials Research Unit, School of Science, King Mongkut's Institute of Technology Ladkrabang, Bangkok 10520, Thailand

*Email: thitiratc@g.swu.ac.th

ABSTRACT

Nowadays, embedding electronic components into fabrics has become increasingly popular in the fabrication of electronic textiles (e-textiles), which has been continuously developed until now [1]. This research focuses on the electrical power generation device that can be used as a power source for electronic components in E-Textiles, namely Triboelectric Nanogenerator (TENG). However, the TENG still has a limitation of losing charge during short time contact-separation which results in low electrical output current. In this work, the TENG device is developed by combination with another energy harvesting technology, namely thermoelectric nanogenerator (TEG) to fabricate a small hybrid energy harvesting device on textiles by using the cotton fabrics composited with polyaniline/carbon nanotube composite (PANI/CNT) and teflon as the main friction materials. The distribution of PANI/CNT composite power in cotton fabric samples was studied by Synchrotron Radiation X-ray Tomographic Microscopy (SR-XTM) technique to confirm PANI/CNT in the internal structure of cotton fabrics by 3D visualization. The important results show that PANI/CNT composite powder was not only dispersed on the surface but also in the internal of cotton fabrics, indicating the percolation threshold for optimum point. At optimum condition, the cotton/PANI/CNT TEG-TENG can provide the maximum output voltage (V_{oc}), output current (I_{sc}), and output power of 40.45 V, 85.34 mA, and 263 μ W respectively. Finally, this work successfully fabricates TEG-TENG as a power supply for small electronic devices relating to use in daily life and we hope this research will be a potential way to develop in future E-textile industry.

REFERENCES

1. A. Komolafe, B. Zaghari, R. Torah, A.S. Weddell, H. Khanbareh, et al., *IEEE Access*, 9, 97152-97179 (2021).

FLEXIBLE SENSOR BASED ON BACTERIAL CELLULOSE – TITANIUM DIOXIDE NANOTUBES COMPOSITE

K.Chaithawee¹, U. Pharino¹, S. Pongampai², T.Maluangnont³ and N. Vittayakorn^{1,*}

¹*Advanced Materials Research Unit, School of Science,
King Mongkut's Institute of Technology Ladkrabang, Bangkok 10520, Thailand*

²*Department of Physics, Faculty of Science,
King Mongkut's University of Technology Thonburi (KMUTT, Bangkok 10140, Thailand*

³*Electroceramics Research Laboratory, College of Nanotechnology,
King Mongkut's Institute of Technology Ladkrabang, Bangkok 10520, Thailand*
Email: Naratip.vi@kmitl.ac.th

ABSTRACT

This research focuses on developing flexible sensors that can be used in daily life and using environmentally friendly materials. Therefore, composites were prepared between bacterial cellulose (BC) and titanium dioxide nanotubes (TNTs). The ratios were changed by 0.5%, 3%, and 10% by volume to study the ratios that affect the properties of the composites. Then the morphology was analyzed by scanning electron microscope (SEM) and the 3D morphology of the BC and TNTs was examined by X-ray tomographic microscopy (XTM) to study the distribution of TNTs used as dispersion phases without the sample being destroyed, the structure and functional groups were investigated by Fourier transform infrared spectroscopy (FTIR) in the range of 400-4000 cm⁻¹. In addition, the crystal structure was analyzed by X-ray diffraction (XRD) technique. The bacterial cellulose was nanofiber with TNTs dispersed on the surface. However, the units cell of BC and HTNTs did not change. Because bacterial cells were flexible, transparent, and biodegradable. We apply these materials to wearable devices, gloves, or other things. This research designed and installed a flexible sensor[1] with a glove to detect resistance. It uses 3 Kirigami[2] patterns to increase stretchability. When measured for resistance, Kirigami pattern 1 had a resistance of 47.35 ohms, which was the highest value compared to pattern 2 and pattern 3. Then take the composite film at various volumes was cut into the first Kirigami pattern and measured for electrical properties, dielectric properties, and the performance of flexible sensors according to sensor variables. The sensors made of composite film at a ratio of 10% by volume showed a Sensitivity of 183.48, %Accuracy of 97.63%, and %Stability of 44.04%, which were the highest values compared to other samples.

REFERENCES

1. S. Huang, Y. Liu, Y. Zhao, Z. Ren, and C. F. Guo, "Flexible electronics: stretchable electrodes and their future," *Advanced Functional Materials*, vol. 29, no. 6, p. 1805924, 2019.
2. P. Won *et al.*, "Stretchable and transparent kirigami conductor of nanowire percolation network for electronic skin applications," *Nano letters*, vol. 19, no. 9, pp. 6087-6096, 2019.

High-resolution X-ray Imaging and Pulse Height Spectra of CeF₃-doped Fluorophosphate Glasses for Scintillator Applications

C.S. Sarumaha^{1,2}, J. Rajagukguk³, N. Chanthima^{1,2}, P. Kidkhunthod⁴,
P. Pakawanit⁴, N. Vittayakorn⁵, P. Kantuptim⁶, T. Yanagida⁶,
J. Kaewkhao^{1,2}

¹Physics Program, Faculty of Science and Technology, Nakhon Pathom Rajabhat University, Nakhon Pathom 73000, Thailand

²Center of Excellence in Glass Technology and Materials Science (CEGM), Nakhon Pathom Rajabhat University, Nakhon Pathom 73000, Thailand

³Department of Physics, Faculty of Mathematics and Natural Sciences, Universitas Negeri Medan, Medan 20221, Indonesia

⁴Synchrotron Light Research Institute, 111 University Avenue, Muang District, Nakhon Ratchasima, 30000 Thailand

⁵Advanced Materials Research Unit, School of Science, King Mongkut's Institute of Technology Ladkrabang, Bangkok 10520, Thailand

⁶Division of Materials Science, Graduate School of Science and Technology, Nara Institute of Science and Technology, 8916-5, Takayama, Ikoma, Nara 630-0192, Japan
Email: chayani.sarumaha@gmail.com

ABSTRACT

We show how fluorophosphate glasses that have been doped with cerium fluoride (CeF₃) can be used as dense scintillators for X-ray imaging. CeF₃-doped 20Li₂O-10AlF₃-2.5CaF₂-(57.5-x)P₂O₅-10Gd₂O₃ with concentration variations (x = 0; 0.05; 0.1; 0.3; 0.5; 1.0; 1.5; 2.0) was prepared and the photoluminescence, X-ray Absorption Near-Edge Structure (XANES), radioluminescence (RL) and decay time were measured. Analysis was done on the scintillation properties, such as pulse height spectra and X-ray imaging. The investigation of X-ray Absorption Near-Edge Structure (XANES) of Ce L_{III}-edge was shown at ~5.718 keV and confirmed the presence of Ce³⁺ and Ce⁴⁺ at ~5.723 keV and ~5.730 keV. The comparison of the Ce³⁺ and Ce⁴⁺ ratios by fitting the energy range in the XANES spectrum may confirm the luminescence characteristic of the glass. A full energy peak was observed in the pulse height spectra of a ²⁴¹Am α-ray irradiation in the PLGdAfCafCe_{0.5} glass, and the calculated light yields of PLGdAfCafCe_{0.5} was 54 Ph/MeV under α-ray. The created glass was successfully imaged with X-rays using a synchrotron light source. From the results, it can be concluded that the PLGdAfCafCe_{0.5} glass showed promising properties as a scintillator application.

Homogenous Zn deposition by fly ash-cellulose separator for high-performance Zn²⁺ batteries

Chengwu Yang¹ and Jiaqian Qin¹

¹ Research Unit of Advanced Materials for Energy Storage, Metallurgy and Materials Science Research Institute, Chulalongkorn University, Bangkok 10330, Thailand
Email: jiaqian.q@chula.ac.th

ABSTRACT

The developed strategies toward stable and dendrite-free Zn anode, including artificial solid-electrolyte interface construction, electrolyte modification and novel separator design, are still unable to satisfy the large-scale commercialization of aqueous zinc-ion batteries, due to the complex preparation process and expensive manufacturing prices [1]. Herein, we fabricated a fly ash-cellulose nanofiber (FACNF) composite separator with the advantages of cost-efficiency and simplified preparation by a facile solution-casting method for dendrite-free Zn anode. The fabricated FACNF separator can efficiently lower the Zn nucleation overpotential, homogeneous the Zn nucleation sites, postpone surface corrosion and promote the uniform Zn deposition, finally realize the high-performance Zn anode. Consequently, compared with pure CNF separator, FACNF separator vastly extends the cycling lifespan of Zn||Zn symmetric cell to 1600h at 2 mA·cm⁻²/1 mAh·cm⁻² and 600h at 5 mA·cm⁻²/2.5 mAh·cm⁻². Moreover, using (NH₄)₂V₁₀O₂₅·8H₂O (NVO) as cathode material, the full cell with FACNF separator shows superior discharge capacity of 79 mAh·g⁻¹ after 4000 cycles at 5 A·g⁻¹, whereas the one with CNF with CNF separator shows low discharge capacity and the abrupt battery failure around 2800 cycles owing to the severe side reactions and dendrite growth. Benefiting from the merits of FACNF in reversibility of Zn plating/stripping, the Zn||NVO pouch cell exhibits a high discharge capacity of 80.5 mAh·g⁻¹ with a high capacity retention of 87.4% after 200 cycles at 0.5 A·g⁻¹. This work provides a low-cost and multi-functional cellulose-based separator for the large-scale commercialization of high-performance AZIBs.

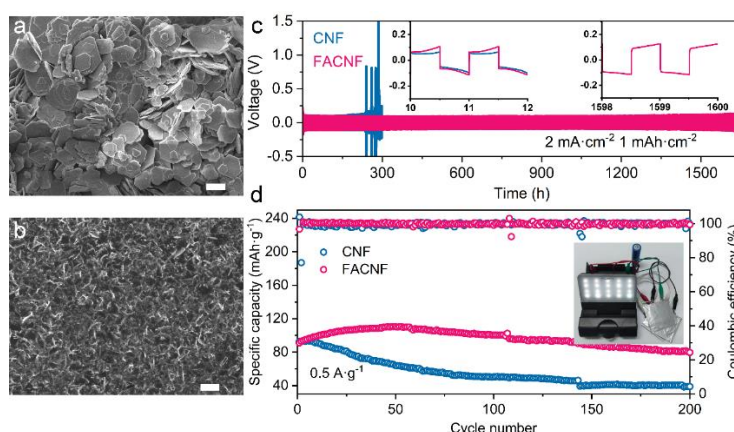


Figure 1. The SEM images of Zn anodes in Zn||Zn symmetric cell with (a) CNF and (b) FACNF separator. (c) The long-term cycling performance of Zn||Zn cells with CNF and FACNF separators. (d) The pouch cells of Zn||NVO full cell using CNF and FACNF separator. Three pouch cells in series can light up a lamp.

REFERENCES

1. C. Yang, X. Zhang, J. Cao, D. Zhang, P. Kidkhunthod, S. Wannapaiboon, J. Qin, ACS Appl Mater Interfaces 2023, 15, 26718.

In Situ X-Ray Absorption Spectroscopy Investigation of Synergistic Effect on Mn-Fe Active Sites in OER and ORR

M. Gopalakrishnan¹, W. Kao-ian¹, W. Lao-atiman² W. Limphirat² and
S. Kheawhom^{1,3*}

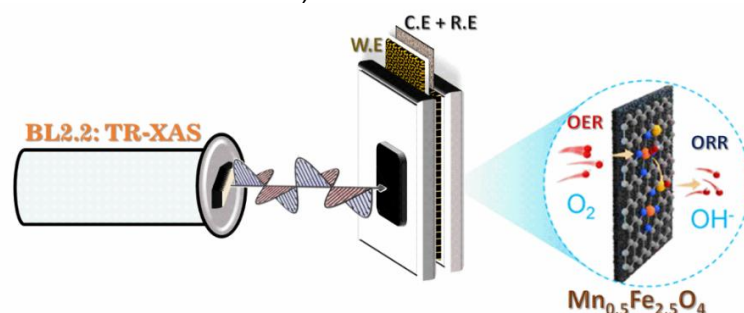
¹Department of Chemical Engineering, Faculty of Engineering, Chulalongkorn University,
Bangkok 10330, Thailand

²Synchrotron Light Research Institute, 111 University Avenue, Muang District, Nakhon
Ratchasima, 30000 Thailand

³Center of Excellence on Advanced Materials for Energy Storage, Chulalongkorn University,
Bangkok 10330, Thailand
Email: Gopalakrishnan.m@chula.ac.th

ABSTRACT

The development and understanding of synergy in clearly defined dual-atom active sites has the potential to support multistep tandem electrocatalytic reactions¹. It is critical to develop a thorough investigation of these reactions intermediate structure and properties through advanced characterization to enhance their electrocatalytic performance^{2,3}. In situ X-ray absorption spectroscopy (XAS) is a potent tool for determining the active sites and structural changes in catalytic materials while they are being used in reactions⁴. Herein, we propose a dual-heteroatom spinel catalyst with adjacent Mn-O and Fe-O active sites for efficient bifunctional 3D electrocatalyst. Operando XAS under practical device operation conditions reveals detailed insights into this dual-atom synergy mechanism for OER and ORR. Atomic information such as valence state, coordination number, and symmetry can be obtained from X-ray absorption near edge structure (XANES) in the energy range that extends 50–100 eV above the absorption edge⁵. The 3D spinel electrocatalyst ($\text{Mn}_{0.5}\text{Fe}_{2.5}\text{O}_4$) has effective catalytic activity for the oxygen reduction reaction ORR ($E_{1/2} = 0.85 \text{ V}$) and the oxygen evolution reaction OER ($\eta_{10} = 210 \text{ mV}@10 \text{ mA cm}^{-2}$).



REFERENCES

- 1 Y. Zhao, D. P. Adiyari Saseendran, C. Huang, C. A. Triana, W. R. Marks, H. Chen, H. Zhao and G. R. Patzke, *Chem. Rev.*, 2023, **123**, 6257–6358.
- 2 M. Gopalakrishnan, M. Etesami, J. Theerthagiri, M. Y. Choi, S. Wannapaiboon, M. T. Nguyen, T. Yonezawa and S. Kheawhom, *Nanoscale*, 2022, **14**, 17908–17920.
- 3 M. Gopalakrishnan, A. A. Mohamad, M. T. Nguyen, T. Yonezawa, J. Qin, P. Thamyingkit, A. Somwangthanaroj and S. Kheawhom, *Mater. Today Chem.*, 2022, **23**, 100632.
- 4 B. Wu, T. Sun, Y. You, H. Meng, D. M. Morales, M. Lounasvuori, A. Beheshti Askari, L. Jiang, F. Zeng, B. Hu, X. Zhang, R. Tai, Z. J. Xu, T. Petit, L. Mai, Y. Zhao, D. P. Adiyari Saseendran, C. Huang, C. A. Triana, W. R. Marks, H. Chen, H. Zhao and G. R. Patzke, *Angew. Chemie Int. Ed.*, 2023, **123**, 6257–6358.

5 X. Liu, G. Zhang, L. Wang and H. Fu, *Small*, 2021, **17**, 2006766.

Investigation of CO₂ hydrogenation on CuFe₂O₄/SBA-15 catalysts via in-situ/operando XAS

W. Yingyuen¹, T. Nanmong¹, W. Obrom¹, K. Deekamwong²,
P. Tawachkultanadilok², J. Wittayakun², S. Prayoonpokarach²,
Y. Poo-arporn³, P. Khemthong⁴, S. Loiha^{1*}

¹Materials Chemistry Research Center, Department of Chemistry, Faculty of Science, Khon Kaen University, Khon Kaen, Thailand

²School of Chemistry, Institute of Science, Suranaree University of Technology, Nakhon Ratchasima, Thailand

³Synchrotron Light Research Institute, 111 University Avenue, Muang District, Nakhon Ratchasima, 30000 Thailand

⁴National Nanotechnology Center (NANOTEC), National Science and Technology Development Agency (NSTDA), Pathumthani 12120, Thailand
Email: Worapol.y@kkumail.com

ABSTRACT

The effective conversion of carbon dioxide (CO₂) into valuable chemicals and fuels has emerged as a crucial approach for mitigating greenhouse gas emissions and utilizing renewable energy sources. A comprehensive study was conducted on the synthesis, characterization, and catalytic performance analysis of CuFe₂O₄/SBA-15 catalysts for CO₂ hydrogenation. The integration of metal ferrite nanoparticles (MFe₂O₄) with mesoporous SBA-15 silica offers numerous advantages, including a high surface area, tunable pore size, and strong metal-support interaction. These catalysts possess unique structural and compositional properties that facilitate efficient CO₂ conversion to valuable chemicals. The catalyst structures were determined mainly by XRD and XAS techniques. Reducibility and the catalytic activity on CO₂ conversion were investigated using an in-situ/operando XAS. The CO₂ conversion directly proceeded without the reduction pretreatment process of CuFe₂O₄/SBA-15. The catalytic conversion and selectivity to CO product increased with increasing temperature. The catalytic activities of CO₂ conversion were strongly affected by the basicity of the catalyst support. These findings pave the way for developing efficient catalyst systems for CO₂ utilization and producing valuable chemicals from CO₂ feedstock. Further investigation is warranted to optimize the catalyst's performance and explore its potential for large-scale applications.

REFERENCES

1. Senamart, N., Loiha, S., Poo-arporn, Y., Tawachkultanadilok, P., Tonlublao, S., Limphirat, W., Duangmanee, S., Kamonpha, P., Wittayakun, J., Osakoo, N., Wannapaiboon, S., & Poo-arporn, R. P. (2021). *In-situ investigation of ethanol steam reforming on Ni and Cr doped ferrites using combined X-ray absorption spectroscopy, mass spectrometry, and gas chromatography*. Radiation Physics and Chemistry, 185, 109492. <https://doi.org/10.1016/j.radphyschem.2021.109492>
2. Fayisa, B. A., Yang, Y., Zhen, Z., Wang, M.-Y., Lv, J., Wang, Y., & Ma, X. (2022). *Engineered Chemical Utilization of CO₂ to Methanol via Direct and Indirect Hydrogenation Pathways: A Review*. Industrial & Engineering Chemistry Research, 61(29), 10319–10335. <https://doi.org/10.1021/acs.iecr.2c00402>
3. Orege, J. I., Kifle, G. A., Yu, Y., Wei, J., Ge, Q., & Sun, J. (2023). Emerging spinel ferrite catalysts for driving CO₂ hydrogenation to high-value chemicals. Matter, 6(5), 1404–1434. <https://doi.org/10.1016/j.matt.2023.03.024>

4. Hou, J., Liu, Y., Weng, R., Li, L., Liu, Y., Sheng, J., & Song, Y. (2022). *Purification of dye-contaminated water using Si-doped mesoporous Fe₃O₄ prepared with rice husk SBA-15 as a template: Behavior and mechanism.* Biomass Conversion and Biorefinery. <https://doi.org/10.1007/s13399-022-02379-3>

Metal-carbon electrocatalysts for oxygen-involving reactions

M. Etesami¹, R. Khezri¹, A. Somwangthanaroj^{1,3,*} and S. Kheawhom^{1,2,3,*}

¹Department of Chemical Engineering, Faculty of Engineering, Chulalongkorn University, Bangkok 10330, Thailand

²Center of Excellence on Advanced Materials for Energy Storage, Chulalongkorn University, Bangkok 10330, Thailand

³Bio-Circular-Green-economy Technology & Engineering Center (BCGeTEC) Faculty of Engineering, Chulalongkorn University, Bangkok 10330, Thailand

Email: mohammad.e@chula.ac.th

ABSTRACT

Oxygen reduction reaction (ORR) and oxygen evolution reaction (OER) are the core of clean energy technology. Oxygen electrocatalysts based on low contents of earth-abundant metals and carbonaceous materials are of prime importance due to their high performance in electrochemical applications [1]. Metal catalysts including nanoparticles to nanoclusters and single atoms have shown excellent results in energy-related reactions, considering the fact that the narrow size distribution of metal particles on carbon reveals a larger surface area of the electrocatalyst. By well-controlling synthesis policies and advanced characterization instruments, the performance of the catalyst associated with the structure at the molecular level is uncovered. Besides the ex-situ characterizations, synchrotron-based analyses can interpret the structure of materials further. X-ray absorption spectroscopy (XAS) comprising X-ray absorption near edge structure (XANES) and extended X-ray absorption fine structure (EXAFS) analysis is analytical techniques that illuminate the local electronic structure of an atom and the oxidation state [2]. In our work, the metal-carbon (FeCo-NC) electrocatalysts were synthesized via sample pyrolysis in N₂ gas. The XAS was used as an advanced technique during the characterization to explain the catalyst structure. The oxidation states of cobalt species is Co^{δ+} in both Co-NC and FeCo-NC. The electrocatalysts exhibited a good performance toward ORR and OER. The optimized electrocatalyst is a good alternative for the cathode application in a zinc-air battery.

REFERENCES

1. M. Etesami, R. Khezri, A. Abbasi, M.T. Nguyen, T. Yonezawa, S. Kheawhom and A. Somwangthanaroj, *Ball mill-assisted synthesis of NiFeCo-NC as bifunctional oxygen electrocatalysts for rechargeable zinc-air batteries, J. Alloys Compd.* **922**, 166287 (2022).
2. B.B. Sarma, F. Maurer, D.E. Doronkin and J.-D. Grunwaldt, *Design of Single-Atom Catalysts and Tracking Their Fate Using Operando and Advanced X-ray Spectroscopic Tools, Chem. Rev.* **123**, 379-444 (2023).

Multi-phase TiO₂ Doped with Ag as a Sensing Material for Nitrite Detection

T. L. Htet¹, S. Pitiphattharabun², R. Techapiesancharoenkij^{1,3}, G. Panomsuwan^{1,3}, N. Pewnim^{1,3}, P. Kidkhumthod⁴, J. Padchasri⁴, O. Jongprateep^{1,3*}

¹Department of Materials Engineering, Faculty of Engineering, Kasetsart University, 50 Ngamwongwan Road, Chatuchak, Bangkok 10900, Thailand

²Program of Sustainable Energy and Resources Engineering, Faculty of Engineering, Kasetsart University, 50 Ngamwongwan Road, Chatuchak, Bangkok 10900, Thailand

³International Collaborative Education Program for Materials Technology, Education, and Research (ICE-Matter), ASEAN University Network/Southeast Asia Engineering Development Network (AUN/SEED-Net), Bangkok 10330, Thailand

⁴Synchrotron Light Research Institute, 111 University Avenue, Muang District, Nakhon Ratchasima 30000, Thailand

*Email: fengotj@ku.ac.th

ABSTRACT

Nitrite salts have been widely used as food preservatives to prevent bacterial growth. However, the excessive presence of nitrites in the human body can lead to gastric and esophageal cancers. Electrochemical sensing is considered a simple, reliable, and effective method for detecting nitrites. In this research, TiO₂ and Ag-doped TiO₂ were utilized as sensing materials for nitrite detection. The synthesis of TiO₂ and Ag-doped TiO₂ was carried out through the solution combustion method. To analyze the phase composition of the synthesized TiO₂ and Ag-doped TiO₂, X-ray diffraction and X-ray absorption near edge structure (XANES) techniques were employed. The diffraction patterns and Ti K-edge XANES spectra indicated that the synthesized powders consisted mainly of anatase, with minor amounts of brookite and rutile. The derivative XANES spectra of Ag-doped TiO₂ suggested that the oxidation state of silver in the Ag-doped TiO₂ powders matched that of AgNO₃. This implies the creation of defects such as oxygen vacancies, which can reduce charge carrier recombination and enhance electron mobility, thereby promoting catalysis. The electrochemical activity of the sensing materials was evaluated using cyclic voltammetry in the presence of sodium nitrite solutions with concentrations ranging from 0.01 mM to 10mM. A significant oxidation reaction was observed at an applied voltage close to 1.4V. Experimental results demonstrated that TiO₂ with a 5 mol% Ag doping exhibited the most notable electrochemical response in the sodium nitrite solution.

REFERENCES

1. Parvizishad, M., et al., *A review of adverse effects and benefits of nitrate and nitrite in drinking water and food on human health*. Health Scope 6, 3 (2017).
2. Bagheri, S., N. Muhd Julkapli, and S. Bee Abd Hamid, *Titanium dioxide as a catalyst support in heterogeneous catalysis*. The Scientific World Journal **2014**, 2014.
3. Luttrell, T., et al., *Why is anatase a better photocatalyst than rutile?-Model studies on epitaxial TiO₂ films*. Scientific Reports 4, 4043 (2014).
4. Cargnello, M., T.R. Gordon, and C.B. Murray, *Solution-phase synthesis of titanium dioxide nanoparticles and nanocrystals*. Chemical Reviews **114**, 9319-9345 (2014).
5. El-Sheikh, S.M., et al., *Tailored synthesis of anatase-brookite heterojunction photocatalysts for degradation of cylindrospermopsin under UV-Vis light*. Chemical Engineering Journal **310**, 428-436 (2017).

Organic-based Three-Phase Composites for Flexible Hybrid Piezoelectric-Triboelectric Nanogenerator

K. Saichompoo¹, A. Naentaeng¹, S. kamcharoen ¹, S. Pongampai², P. Pakawanit³, N. Vittayakorn⁴ and T. Charoonsuk^{1*}

¹Department of Materials Science, Faculty of Science, Srinakharinwirot University, Sukhumvit 23, Watthana, Bangkok 10110, Thailand

²Department of Physics, Faculty of Science, King Mongkut's University of Technology Thonburi, Bangkok 10140, Thailand

³Synchrotron Light Research Institute (Public Organization), 111 University Avenue, Muang District, Nakhon Ratchasima 30000, Thailand

⁴Advanced Materials Research Unit, School of Science, King Mongkut's Institute of Technology Ladkrabang, Bangkok 10520, Thailand

*Email: thitiratc@g.swu.ac.th

ABSTRACT

A small power supply for wearable/portable electronics has been gain much attention. Even though a wide variety of synthetic materials can be used, concerning about the electronic wastes and toxic restrict the application in field of biomedical devices [1]. In this work, flexible triboelectric nanogenerators (F-TENGs) were fabricated by using of chitosan (CS) biopolymers as contact layer and composite with the bacterial cellulose (BC) to increase the contact area. The electrical output is further enhanced by adding the organic piezoelectric triglycine sulfate (TGS). By considering the crucial point of percolation threshold, the morphology and particle distribution study is necessary. It was investigate by scanning electron microscopy (SEM), atomic force microscope (AFM) and synchrotron radiation x-ray thermography (SR-XTM). The 3D distribution from SR-XTM can help for pointing out the best condition. The 5wt% of TGS in the CS/BC composite can reach maximum output voltage (Voc) of 38.4 V, output current (Isc) 0.211 μ A, which is higher than that of CS/BC composite due to increasing the number of electric charges by contact between device and the piezoelectric effect. The authors are confident that this study will provide a new approach to improve the electrical output of flexible hybrid piezoelectric/triboelectric nanogenerator that can be used in contact with human body to drive the portable and wearable electronics in medical device industry in future.

REFERENCES

1. Petritz A, Karner-Petritz E, Uemura T, Schäffner P, Araki T, Stadlober B, et al. Imperceptible energy harvesting device and biomedical sensor based on ultraflexible ferroelectric transducers and organic diodes. Nature Communications. 2021;12(1):2399.

Oxidation State of Fe in Volcanic Rocks of Thailand as Potential Raw Materials for Mars Regolith Simulant

N. Apisuk¹, S. Paisarnsombat¹, W. Chancharoen², and C. Saiyasombat³

¹*Department of Earth Sciences, Faculty of Science, Kasetsart University, Bangkok, 10900, Thailand*

²*Princess Srisavangavadhana College of Medicine, Faculty of Science, Chulabhorn Royal Academy, Bangkok, 10210, Thailand*

³*Synchrotron Light Research Institute (Public Organization), Nakhon Ratchasima 30000, Thailand*

Email: naphat.apis@ku.th

ABSTRACT

Martian Regolith Simulants are a terrestrial material used to simulate the chemical and mechanical properties of Martian regolith for research, experiments, and prototype testing activities related to Martian regolith. Raw materials of the simulants are basaltic rocks and other volcanic rocks [1]. Forty-two rock samples were collected from Lopburi, Phetchabun, Chantaburi, Sa Kaeo, and Trat provinces. Chemical compositions and mineralogy of volcanic rocks have previously been studied and classified. Compared to Martian soil and Mars Regolith Simulants databases, the rock samples have lower FeO_t. Adding amounts of magnetite and hematite is necessary to develop Mars Regolith Simulant. Thus, this study aims to study the oxidation state of Fe in volcanic rocks using X-ray Absorption Near Edge Structure (XANES) with an on-the-fly scanning technique. The eighteen samples representing eighteen study sites were mechanically crushed using Los Angeles Abrasion Machine. The XANES were collected from Fe K-edge. The Fe foil, ferrous oxide, and ferric oxide were used as standards for energy calibration at 7112 eV, 7119.07 eV, and 7123.41 eV, respectively. The oxidation state was determined by comparing binding energy (E_0) to standards [2]. Using the Athena software, the binding energy was calculated from the first derivative method of the normalized XANES absorption spectra. The XAS results indicate that Fe in the samples are mixed between ferrous (Fe²⁺) and ferric (Fe³⁺) ions. Rock samples also have been analyzed using X-ray Diffraction (XRD) and X-ray Fluorescence (XRF) using synchrotron radiation, which provides intense and tunable X-ray beams. The results suggest that Sa Kaeo basalt is likely a potential raw material for developing Thailand Mars Regolith Simulant. However, further studies on the physical and geotechnical properties of the samples are recommended.

REFERENCES

1. X. Zeng et al., *JMSS-1: a new Martian soil simulant*, Earth Planet, 2015, Sp 67, 72.
2. S. Paisarnsombat et al., Characteristic of Fe in tektite observed from XANES and UV-Vis spectroscopy, J. Phys.: Conf., 2021, Ser. 1719 012002.

Physical and Photoluminescence Investigation of Eu³⁺ Doped Gadolinium Borate Scintillating Glass

B. Damdee¹, K. Kirdsiri^{1,2}, H.J. Kim³, K. Yamanoi⁴, N. Wongdamnern⁵,
P. Kidkhunthod⁶, R. Raja Ramakrishna², J. Kaewkhao^{1,2}

¹Physics program, Faculty of Science and Technology, Nakhon Pathom Rajabhat University, Nakhon Pathom, 73000, Thailand

²Center of Excellence in Glass Technology and Materials Science (CEGM), Nakhon Pathom Rajabhat University, Nakhon Pathom, 73000, Thailand

³Department of Physics, Kyungpook National University, Deagu 702-701, Republic of Korea

⁴Institute of Laser Engineering, Osaka University, 2-6 Yamadaoka, Suita, Osaka 565-0871, Japan

⁵Faculty of Science and Technology, Rajamangala University of Technology Suvarnabhumi, Nonthaburi, 11000 Thailand

⁶Synchrotron Light Research Institute, Nakhon Ratchasima, 30000, Thailand
Email: benchaphorn@npru.ac.th

ABSTRACT

The bright reddish-orange emitting Eu³⁺-doped gadolinium borate glasses of 25Gd₂O₃-(75-x) B₂O₃-xEu₂O₃ (GdBEu) (x = 0.1, 0.3, 0.5, 1.0, 3.0, 5.0, 7.0, and 9.0 mol%) were fabricated by melt-quenching technique at 1400 °C for 3 hours. All GdBEu glasses were investigated the photoluminescence, scintillation, and lasing potential properties. The energy transfers processes from Gd³⁺→Eu³⁺ in these glasses were discovered. Photons in the ultraviolet, visible, and near-infrared region wavelengths were absorbed by glasses. The photoluminescence excitations were performed at 275 nm and 394 nm, respectively. When the energy transferred from Gd³⁺ to Eu³⁺, luminescence features revealed an intense red emission with a wavelength of 614 nm (⁵D₀ → ⁷F₂). The glass is optimum Eu³⁺ ion concentration was 7.0 mol%, corresponding to the maximum emission intensity. Judd-Ofelt parameters were calculated from the emission spectra and the radiative properties of several excited states were examined, including the transition probability (A_R), branching ratio (β_R), stimulated emission cross-section (σ_e), and decay time (τ_R). Once the Eu³⁺ concentration increased from 0.1 to 9.0 mol%, the decay time of the ⁵D₀ level dropped from 1.824 ms to 1.585 ms. The colors of glasses were confirmed by the Commission internationale de l'éclairage (CIE) chromaticity diagram. The glass samples had a peak area of radioluminescence (RL) spectrum 18% of BGO scintillation crystal.

REFERENCES

1. Aryal, P., Kim, H.J., Khan, A., Saha, S., Kang, S.J., Kothan, S., Yamsuk, Y., Kaewkhao, J., 2020. Development of Eu³⁺-doped phosphate glass for red luminescent solid-state optical devices. *J. Lumin.* 227, 117564. <https://doi.org/10.1016/j.jlumin.2020.117564>
2. De, M., Jana, S., 2020. Optical characterization of Eu³⁺ doped titanium barium lead phosphate glass. *Optik (Stuttg)*. 215, 164718. <https://doi.org/10.1016/j.ijleo.2020.164718>
3. Farias, A.M., Sandrini, M., Viana, J.R.M., Baesso, M.L., Bento, A.C., Rohling, J.H., Guyot, Y., De Ligny, D., Nunes, L.A.O., Gandra, F.G., Sampaio, J.A., Lima, S.M., Andrade, L.H.C., Medina, A.N., 2015. Emission tunability and local environment in europium-doped OH-free calcium aluminosilicate glasses for artificial lighting applications. *Mater. Chem. Phys.* 156, 214–219. <https://doi.org/10.1016/j.matchemphys.2015.03.002>
4. Gandhi, Y., Rajanikanth, P., Sundara Rao, M., Ravi Kumar, V., Veeraiah, N., Piasecki, M., 2016. Effect of tin ions on enhancing the intensity of narrow luminescence line at 311 nm of Gd³⁺ ions in Li₂O-PbO-P₂O₅ glass system. *Optical Materials* 57, 39-44

5. Han, L., Zhang, Q., Song, J., Xiao, Z., Qiang, Y., Ye, X., You, W., Lu, A., 2020. A novel Eu³⁺-doped phosphate glass for reddish orange emission: Preparation, structure and fluorescence properties. *J. Lumin.* 221, 117041. <https://doi.org/10.1016/j.jlumin.2020.117041>
6. Kaewnuam, E., Kaewkhao, J., 2018. Synthesis-temperature effect on the luminescence under light and UV excitation of Eu³⁺ doped lithium lanthanum borate phosphor. *Mater. Today Proc.* 5, 15086–15091. <https://doi.org/10.1016/j.matpr.2018.04.062>
7. Kalpana, T., Gandhi, Y., Sanyal, B., Sudarsan, V., Bragieli, P., Piasecki, M., Ravi Kumar, V., Veeraiah, N., 2015. Influence of alumina on photoluminescence and thermoluminescence characteristics of Gd³⁺ doped barium borophosphate glasses. *J. Lumin.* 15, 30777–8. <http://dx.doi.org/10.1016/j.jlumin.2016.06.053>
8. Kalpana, T., Brik, M.G., Sudarsan, V., Naresh, P., Ravi Kumar, V., Kityk, I.V., Veeraiah, N. 2015. Influence of Al³⁺ ions on luminescence efficiency of Eu³⁺ ions in barium boro-phosphate glasses. *J. Non. Cryst. Solids* 419, 75–81.
9. Kal, T., Brik, M.G., Sudarsan, V., Naresh, P., Ravi Kumar, V., Kityk, I.V., Veeraiah, N. 2015. Influence of Al³⁺ ions on luminescence efficiency of Eu³⁺ ions in barium boro-phosphate glasses. *J. Non. Cryst. Solids* 419, 75–81.
10. Khan, I., Rooh, G., Rajaramakrishna, R., Sirsittapokakun, N., Kim, H.J., Kaewkhao, J., Kirdsiri, K. 2018. Energy transfer phenomenon of Gd³⁺ to excited ground state of Eu³⁺ ions in Li₂O-BaO-Gd₂O₃-SiO₂-Eu₂O₃ glasses. *Spectrochimica Acta Part A: Molecular and Biomolecular Spectroscopy.* 18, 30999–5
11. Kravets, V.A., Ivanova, E. V., Orekhova, K.N., Petrova, M.A., Gusev, G.A., Trofimov, A.N., Zamoryanskaya, M. V., 2020. Synthesis and luminescent properties of bismuth borosilicate glass doped with Eu³⁺. *J. Lumin.* 226, 117419. <https://doi.org/10.1016/j.jlumin.2020.117419>
12. Lin, H., Chen, D., Yu, Y., Yang, A., Zhang, R., Wang, Y., 2012. Ultraviolet upconversion luminescence of Gd³⁺ and Eu³⁺ in nano-structured glass ceramics. *Mater. Res. Bull.* 47, 469–472. <https://doi.org/10.1016/j.materresbull.2011.10.021>
13. Ramachari, D., Rama Moorthy, L., Jayasankar, C.K., 2013. Phonon sideband spectrum and vibrational analysis of Eu³⁺ -doped niobium oxyfluorosilicate glass. *J. Lumin.* 143, 674–679. <https://doi.org/10.1016/j.jlumin.2013.05.025>
14. Ramesh, P., Hegde, V., Pramod, A.G., Eraiah, B., Agarkov, D.A., Eliseeva, G.M., Pandey, M.K., Annapurna, K., Jagannath, G., Kokila, M.K., 2020. Compositional dependence of red photoluminescence of Eu³⁺ ions in lead and bismuth containing borate glasses. *Solid State Sci.* 107, 106360. <https://doi.org/10.1016/j.solidstatesciences.2020.106360>
15. Ramteke, D.D., Gedam, R.S., 2014. Luminescence properties of Gd³⁺ containing glasses for ultra-violet (UV) light. *J. Rare Earths* 32, 389–393. [https://doi.org/10.1016/S1002-0721\(14\)60082-X](https://doi.org/10.1016/S1002-0721(14)60082-X)
16. Shimizugawa, Y., Umesaki, N., Hanada, K., Sakai, I., Craft, P., Plaza, K., 2001. amorphous, glass and liquids X-ray induced reduction of rare earth ion t t t (Arbitrary Unit) t t t (Arbitrary Unit) μ • t t t (Arbitrary Unit) μ • Energy 797–799.
17. Sormlar, W., Choeycharoen, P., Wannagon, A., 2020. Characterization of alumina crucible made from aluminum industrial waste. *Journal of the Australian Ceramic Society.* 56, 771–779.
18. Steinbrück, J., Nolte, P.W., Schweizer, S., 2020. Far-field studies on Eu³⁺-doped lithium aluminoborate glass for LED lighting. *Opt. Mater. X* 5, 2–6. <https://doi.org/10.1016/j.omx.2019.100046>
19. Swetha, B.N., Keshavamurthy, K., Jagannath, G., 2021. Influence of size of Ag NP on spectroscopic performances of Eu³⁺ ions in sodium borate glass host. *Optik (Stuttg).* 240, 166918. <https://doi.org/10.1016/j.ijleo.2021.166918>
20. Ullah, I., Rooh, G., Khattak, S.A., Kothan, S., Kaewkhao, J., Khan, I., 2021. Effective red-orange luminescence and energy transfer from Gd³⁺ to Eu³⁺ in lithium gadolinium magnesium borate for optical devices. *Journal of Non-Crystalline Solids.* 569, 120927
21. Venkatramu, V., Navarro-Urrios, D., Babu, P., Jayasankar, C.K., Lavín, V., 2005. Fluorescence line narrowing spectral studies of Eu³⁺-doped lead borate glass. *J. Non. Cryst. Solids* 351, 929–935. <https://doi.org/10.1016/j.jnoncrysol.2005.02.010>
22. Vijayalakshmi, L., Naveen Kumar, K., Hwang, P., 2019. Dazzling red luminescence dynamics of Eu³⁺ doped lithium borate glasses for photonic applications. *Optik (Stuttg).* 193, 163019. <https://doi.org/10.1016/j.ijleo.2019.163019>
23. Wu, Z., Wu, H., Tang, L., Li, Y., Xiaochun, D., Guo, Y., 2017. Fluorescence and energy transfer between Eu³⁺ and Sm³⁺ in single doped and co-doped borate glass. *J. Non. Cryst. Solids* 463, 169–174. <https://doi.org/10.1016/j.jnoncrysol.2017.03.010>
24. Yang, Y., Yang, Z., Chen, B., Li, P., Li, X., Guo, Q., 2009. Spectroscopic properties and thermal stability of Er³⁺-doped germanate-borate glasses. *J. Alloys Compd.* <https://doi.org/10.1016/j.jallcom.2009.01.096>
25. Yu, C., Zhang, Xizhen, Li, X., Zhang, J., Xu, S., Zhang, Xiangqing, Zhang, Y., Wang, X., Wang, L., Sui, G., Chen, B., 2019. Determination of Judd-Ofelt parameters for Eu³⁺-doped alkali borate glasses. *Mater. Res. Bull.* 120, 110590. <https://doi.org/10.1016/j.materresbull.2019.110590>

Platinum and PtNi nanoparticle-supported multiwalled carbon nanotube electrocatalysts prepared by one-pot pyrolytic synthesis with an ionic liquid for dye-sensitized solar cells

T. Sanjailuk¹, K. Pan², and P. Hasin^{1*}

¹*Department of Chemistry, Faculty of Science, Kasetsart University, Bangkok, Thailand*

²*School of Chemistry and Materials Science, Heilongjiang University, Harbin, China*

**E-mail: fscipths@ku.ac.th*

ABSTRACT

With an aim of enhancing the power conversion efficiency (PCE), a nanocomposite comprising of PtNi₃ nanoparticles (NPs) and multiwalled carbon nanotubes (MWCNTs) synthesized using one-pot pyrolysis of nickel-based bis(trifluoromethyl sulfonyl) imide ([Tf₂N]) ionic liquid (IL), platinum precursor, and MWCNTs was explored as a promising candidate for the CE in DSSCs. The photovoltaic measurement confirmed that this composite electrode showed better electrocatalytic activity toward the tri-iodide reduction reaction compared with typical Pt and Pt/MWCNT electrodes. We found that the alloy formation by Ni modification affects the electrocatalytic activity. Consequently, the greater efficiency of DSSC was achieved for PtNi₃/MWCNT CE compared to Pt and Pt/MWCNT CEs, which was attributed to the rapid charge transfer, high electrical conduction, and excellent electrocatalysis. The DSSC using PtNi₃/MWCNT CE yielded PCE of 9.13%, which was higher than those using the Pt (7.84%) and Pt/MWCNT (8.69%) CEs. The experimental results concluded the potential of PtNi₃/MWCNTs to be used as the CE in DSSCs due to the high PCE, low cost in combination with simple preparation, and scalability.

Rayon Fabric-P3HT composite for High Efficient Triboelectric-Thermoelectric Nanogenerator

C. Sae-tang¹, S. Navatragulpisit¹, P. Maosom¹, S. Pongampai²,
P. Pakawanit³, S. Sriphan⁴, N. Vittayakorn⁵ and T. Charoonsuk^{1*}

¹Department of Materials Science, Faculty of Science, Srinakharinwirot University,
Sukhumvit 23, Watthana, Bangkok 10110, Thailand

²Department of Physics, Faculty of Science, King Mongkut's University of Technology
Thonburi, Bangkok 10140, Thailand

³Synchrotron Research and Applications Division, Synchrotron Light Research Institute, 111
University Avenue, Muang District, Nakhon Ratchasima, 30000, Thailand

⁴Faculty of Science, Energy and Environment, King Mongkut's Institute of Technology
Ladkrabang, Bangkok 10520, Thailand

⁵Advanced Materials Research Unit, School of Science, King Mongkut's Institute of
Technology Ladkrabang, Bangkok 10520, Thailand

*Email: thitiratc@g.swu.ac.th

ABSTRACT

The electronic devices embedding in fabrics has become increasingly attention for textile technologies to be connected with the internet and other wireless system. One of essential requirement is to search or fabricate an external power source within high flexibility and lightweight. This research interest in a small power generation device that can be harvest the energy in ambient condition for powering the small electronics, namely thermoelectric-triboelectric hybrid nanogenerator (TEG-TENG). The authors fabricated rayon fabrics as main contact layer with developing and enhancing the electrical output efficiency by compositing with poly(3-hexylthiophene) (P3HT) [1]. Moreover, the contact efficiency with high electrical conductivity was modified within the cotton/CNT composite. Synchrotron Radiation X-ray Tomographic Microscopy (SR-XTM) technique is important methodology to determine the percolation threshold relative to the suitable amount used for fabrication. Finally, the output performance is determined by oscilloscope and digital multimeter and found to be 15 V for open circuit voltage (V_{OC}) and 15.9 μA for short circuit current (I_{SC}). The authors hope this research will be useful for the development of hybrid nanogenerator devices that can be used by combination with electronic textile industry.

REFERENCES

1. S Bonardd, S Morales N, Gence L, Sald días C, Angel FA, Kortaberria G, et al., *appl. Mater. Interfaces*, 12,13275-13286 (2020).

Relationship of crystallization behavior by In-situ synchrotron wide-angle X-ray scattering and resistant starch formation of debranched cassava starches

A. Dongdang¹, W. Kiatpongarp², S. Soontaranon², and S. Tongta^{1*}

¹*School of Food Technology, Institute of Agricultural Technology, Suranaree University of Technology, Nakhon Ratchasima, Thailand.*

²*Synchrotron Light Research Institute (Nakhon Ratchasima, Thailand.)
E-mail: atcharadongdang@gmail.com*

ABSTRACT

The native and waxy cassava starch suspensions (15 % w/w) were debranched at 55 °C for 4 and 5 h. The crystallization behavior monitored using in-situ synchrotron wide-angle x-ray scattering (WAXS) during incubation at low (15 & 25 °C), intermediate (45 °C), and high (65 & 85°C) temperature. Avrami equation was used to quantify the crystallization kinetics of debranched starch. The relationship of crystallinity, crystal size and resistant starch content of incubated debranched starches were considered.

A WAXS pattern of B-type was developed during debranching of native cassava starch for 4 h while the crystallization of waxy cassava starch did not occur. During incubation, low temperature and extra-long chains favored the B-type crystalline structure while A-type crystalline was promoted by high temperature and short chains. At low incubation temperature (15 and 25°C), the two-stage crystallization was developed which was a rapid rate during cooling and slow rate during incubation period. For the intermediate temperature (45 °C), the single-stage crystallization was observed. The crystallization rate at lower temperature was faster than at the higher temperature for both debranched normal and waxy starches. An increase in crystallinity was associated with a larger lateral crystal size. The low-temperature incubation had smaller lateral crystal size than that intermediate-temperature incubation. An increase in crystallinity or crystal size was associated with a higher resistant starch content for the same type of debranched starch.

Remineralizing effect of nanohydroxyapatite-containing varnish on artificial enamel lesion

C. Toejamsee, T. Thaweepanyopas, N.Phonarcha, W. Nakarungkul, W. Ariyakriangkai, and S. Cheewakriengkrai¹

*The Faculty of Dentistry, Chiang Mai University, Sutep Road, Suthep Subdistrict, Muang District, Chiang Mai Province 50200, Thailand
Email: noppphon2554@gmail.com*

ABSTRACT

Dental varnish is oral remineralizing agent which presents strong potential for dental caries prevention [1]. Meanwhile, nanohydroxyapatite is a bioactive material that induces a remineralizing effect on tooth surfaces and is widely used in the dental field nowadays [2]. However, there are no relevant studies involving nanohydroxyapatite containing into dental varnish form. Furthermore, mineral investigation needs Synchrotron radiation to evidently illustrate the mineral transformation on tiny tooth specimens. This advance technology performs 3D volumetric analysis as well as micromorphological examination on applied tooth surfaces [3]. Thus, this study aims to compare the remineralization potential through the percentage gain of calcium and phosphorus as well as calcium/phosphorus ratio which change after the intervention between fluoride varnish and nanohydroxyapatite-containing varnish. Thirty 3x2 mm enamel specimens were obtained from human molars. All specimens were immersed in a demineralizing solution for 14 days to mimic artificial enamel lesions and then divided into three groups (N=10): free active agent varnish (control), nanohydroxyapatite-containing varnish (Faculty of Science, CMU, Chiang Mai, Thailand) and fluoride varnish (DuraphatTM, Woelm Pharma Co., Eshwege, Germany). All specimens were simulated in the pH cycle for 7 days. A scanning electron microscope with energy dispersive X-ray (SEM/EDX) and Synchrotron radiation X-ray tomographic microscopy (SRXTM, BL1.2W) technique were used for the evaluation of the remineralizing effect and micromorphological analysis. The results were statistically analyzed by one-way ANOVA and paired t-test ($P<0.05$). It showed a statistically significant difference in the percentage gain of both calcium and phosphorus after applying nanohydroxyapatite-containing varnish and fluoride varnish ($P<0.05$). Meanwhile, the mean of the percentage gain of both calcium and phosphorus along with calcium/phosphorus ratio that increased in nanohydroxyapatite-containing varnish was not different from fluoride varnish. In conclusion, the increasing percentage gain of both calcium and phosphorus as well as calcium/phosphorus ratio in nanohydroxyapatite-containing varnish was not different from fluoride varnish.

REFERENCES

1. Mishra P, Fareed N, Battur H, Khanagar S, Bhat MA, Palaniswamy J. Role of fluoride varnish in preventing early childhood caries: A systematic review. *Dent Res J (Isfahan)*. 2017;14(3): 169-76.
2. Pepla E, Besharat LK, Palaia G, Tenore G, Migliau G. Nano-hydroxyapatite and its applications in preventive, restorative and regenerative dentistry: a review of literature. *Ann Stomatol (Roma)*. 2014;5(3): 108-14.
3. Kantrong N, Khongkaphet K, Sitornsud N, Lo-apirukkul P, Phanprom W, Rojviriya C, et al. Synchrotron radiation analysis of root dentin: The roles of fluoride and calcium ions in hydroxyapatite remineralization. *J Synchrotron Radiat*. 2022;29(2): 496–504.

Selective acetylene removal from ethylene-rich feed by cross-metathesis over supported WO₃ catalysts

P. Promchana^{1,2}, K. Choojun^{1,2}, and T. Sooknoi^{1,2}

¹*Department of Chemistry, Faculty of Science, King Mongkut's Institute of Technology
Ladkrabang, Chalongkrung Road, Ladkrabang, Bangkok, 10520, Thailand*

²*Catalytic Chemistry Research Unit, Faculty of Science, King Mongkut's Institute of
Technology Ladkrabang, Chalongkrung Road, Ladkrabang, Bangkok, 10520, Thailand
Email: im.pratya@gmail.com, kittisak.ch@kmitl.ac.th*

ABSTRACT

Acetylene in ethylene-rich feed can be removed via acetylene/ethylene cross-metathesis over WO₃-supported catalysts at 450 °C, yielding 1,3-butadiene with cyclohexene as a minor product. The catalyst must be treated with ethylene at 600 °C to generate a genuinely active site of tungsten (IV) alkylidene species (W=CH₂). The H₂ treatment decreases surface W=O concentration, and hence the activity. Raman spectroscopy shows that active dioxo-WO₃ ((O=)₂W(O-Si)₂) was generated in 2%WO₃/SiO₂, while the WO₃ cluster and bulk WO₃ exist in 3-5%WO₃/SiO₂ and 7%WO₃/SiO₂, respectively. The 5%WO₃/NaX and 5%WO₃/NaY provide lower activity due to coke formation over the acid sites. With high surface area and confined surface silanol of 5%WO₃/MCM-41 and 5%WO₃/SBA-15, in situ TR-EXAFS evidences the formation of mono-oxo WO₃ species with 4-oxygen coordination (O=W(O-Si)₃). This species provides an isolated W=CH₂ site with relatively higher activity and is less prone to coke formation than the WO₃ cluster in 5%WO₃/SiO₂.

REFERENCES

1. P. Promchana, K. Choojun, Y. Poo-arporn and T. Sooknoi, *Applied Catalysis A: General*, 2023, pp. 118972.

Solar-light-driven photocatalytic degradation of organic pollutants in wastewater by using heterojunction photocatalyst

T. Senasu, T. Chankhanittha, and S. Nanan

Department of Chemistry, Faculty of Science, *Khon Kaen University*, 123 Mitraparb Road,
Muang District, Khon Kaen,
40002 Thailand
Email: suwatna@kku.ac.th

ABSTRACT

Promising Promising strategy to fabricate visible-light-responsive photocatalysts is a challenging research topic in photocatalysis. In this talk, various heterojunctions including ZnO/Bi₂MoO₆, CdS/BiOBr, ZnO/ZnS, , and ZnO/CdS will be presented. Basically, the hydrothermal/solvothermal method was used for creation of the individual photocatalyst with the advantages of inexpensive, easy to control, and high yield of the product. After that the binary and ternary heterojunction photocatalysts were fabricated. The synthesized photocatalysts were characterized by using numerous techniques such as XRD, FT-IR, SEM, TEM, XPS, XAS and PL. The results confirmed that prepared heterojunctions showed enhance photocatalytic performance in comparison to those of the pristine photocatalysts. The photoactivity toward degradation of azo dyes (reactive red 141, Congo red) and antibiotics (ofloxacin, norfloxacin, oxytetracycline) under natural sunlight was reported. The generation heterostructure photocatalysts enhances the photocatalytic performance by suppressing the recombination of electron-hole pairs at the interface. The photodegradation of the pollutants followed pseudo-first order kinetics. The photocatalyst showed structural stability after seven cycles. The crucial species involved in the degradation of the pollutants was also investigated. Charge transfer at the prepared heterojunction is proposed. These works in our group provide a facile strategy for the interfacial engineering of sunlight-active heterojunctions with enhanced photocatalytic performance for environmental remediation.

REFERENCES

1. T. Senasu, T. Chankhanittha, K. Hemaibool and S. Nanan, *Mater Sci. in Semicon. Proc.* **123**, 10558 (2021).
2. T. Senasu, S. Nijpanich, S. Juabrum, N. Chanlek, and S. Nanan, *App. Sur. Sci.* **567**, 150850 (2021).

Stable and Efficient Dopant-free P3HT-based Perovskite Solar Cell for Indoor Application via Organometallic Interlayer

C. Seriwattanachai¹, S. Sahasithiwat², T. Chotchuangchutchaval³,
W. Wattanathana⁴, A. Kaewprajak⁵, L. Srathongsian¹, T. Sukwiboon¹,
A. Inna¹, N. Phuphathanaphong¹, K. K. S. Thant¹, R. Supruangnet⁶,
H. Nakajima⁶, P. Kumnorkaew⁵, D. Wongratanaphisan⁷,
P. Pakawatpanurut^{8,9}, P. Ruannkham⁷ and P. Kanjanaboos^{1,8,*}

¹School of Materials Science and Innovation, Faculty of Science, Mahidol University, Nakhon Pathom 73170, Thailand

²National Metal and Materials Technology Center (MTEC), National Science and Technology Development Agency (NSTDA), 114 Thailand Science Park, Phahonyothin Road, Khlong Luang, Pathum Thani 12120, Thailand

³King Mongkut's University of Technology North, Department of Industrial Engineering Technology, Bangkok 10800, Thailand

⁴Department of Materials Engineering, Faculty of Engineering, Kasetsart University, Ladyao, Chatuchak, Bangkok 10900,

⁵National Nanotechnology Center (NANOTEC), National Science and Technology Development Agency (NSTDA), 114 Thailand Science Park, Phahonyothin Road, Khlong Luang, Pathum Thani 12120, Thailand

⁶Synchrotron Light Research Institute, 111 University Avenue, Muang District, Nakhon Ratchasima, 30000 Thailand

⁷Department of Physics and Materials Science, Faculty of Science, Chiang Mai University, Chaing Mai 50200, Thailand

⁸Center of Excellence for Innovation in Chemistry (PERCH-CIC), Ministry of Higher Education, Science, Research and Innovation, Bangkok 10400, Thailand

⁹Department of Chemistry and Center of Sustainable Energy and Green Materials, Faculty of Science, Mahidol University, Bangkok, 10400, Thailand
Email: pongsakorn.kan@mahidol.edu

ABSTRACT

Perovskite solar cell (PSCs) has been invented in 2008 with power conversion efficiency (PCE) at 3.8%. [1] By incorporating 2,20,7,70 - tetrakis[N,N-di(4-methoxyphenyl)amino]-9,90 -spirobifluorene (spiro-OMeTAD) as hole transporting material (HTM), the performance of spiro-based PSCs surpassed 9.7% under one sun in 2012. [2] Spiro-OMeTAD is commonly doped with 4-tert-Butylpyridine (tBP) and Lithium bis(trifluoromethylsulfonyl)-imide (Li-TFSI) to gain superior conductivity and solar cell performance by reducing ionization energy at the cost of lower stability. Furthermore, spiro-OMeTAD is sensitive to moisture and oxygen, leading to degradation of the whole perovskite devices. [3] As a consequence, a dopant-free hole transport material is crucial for future stable and efficient PSCs. Poly(3-hexylthiophene) (P3HT) has been introduced as an interesting dopant-free HTM due to its π - π stacking molecular structure and hydrophobic surface. The π - π stacking structure between each thiophene rings can be observed by a shift in sulfur's binding energy to a higher value in X-ray photoelectron spectroscopy (XPS). Nevertheless, high surface energy difference between perovskite and P3HT layer leads to poor contact and reduced charge transportation. This obstacle can be overcome through a simple surface

modification on perovskite surface via a molecular bridge strategy to achieve a champion PCE over 30% under 1000 lux indoor light. In this study, organometallic interface modification was developed to boost solar cell performance and stability under 1-sun and 1000 lux indoor light irradiation. To gain deeper insights, ultraviolet photoelectron spectroscopy (UPS) has been utilized to identify work functions of the P3HT thin films with and without the interface modification, while photoemission electron microscopy (PEEM) reveals work function distributions on the surfaces.

REFERENCES

1. A. Kojima, K. Teshima, Y. Shirai, and T. Miyasaka, "Organometal Halide Perovskites as Visible-Light Sensitizers for Photovoltaic Cells," *Journal of the American Chemical Society*, vol. 131, no. 17, pp. 6050-6051, 2009/05/06 2009, doi: 10.1021/ja809598r.
2. H. S. Kim *et al.*, "Lead iodide perovskite sensitized all-solid-state submicron thin film mesoscopic solar cell with efficiency exceeding 9%," (in eng), *Sci Rep*, vol. 2, p. 591, 2012, doi: 10.1038/srep00591.
3. G. Tumen-Ulzii *et al.*, "Understanding the Degradation of Spiro-OMeTAD-Based Perovskite Solar Cells at High Temperature," *Solar RRL*, vol. 4, no. 10, p. 2000305, 2020, doi: <https://doi.org/10.1002/solr.202000305>.

Structural characterization and XANES spectra of aluminium potassium gadolinium phosphate glasses doped with Er₂O₃

P. Thongyoy¹, C. Kedkaew¹, P. Meejitpaisan^{2,3}, P. Kidkhunthod⁴,
R. Rajaramakrishna⁵, and J. Kaewkhao^{2,3}

*¹Department of Physics, Faculty of Science, King Mongkut's University of Technology
Thonburi, Bangkok 10140, Thailand*

*²Center of Excellence in Glass Technology and Materials Science (CEGM), Nakhon Pathom
Rajabhat University, Nakhon Pathom 73000, Thailand*

*³Physics Program, Faculty of Science and Technology, Nakhon Pathom Rajabhat University,
Nakhon Pathom 73000, Thailand*

*⁴Synchrotron Light Research Institute (Public Organization), 111 University Avenue, Muang,
Nakhon Rattchaisima, 30000, Thailand*

*⁵Department of Post Graduate Studies and Research in Physics, The National College,
Jayanagar, Bengaluru 560070, Karnataka, India
Email: phalada.izee@mail.kmutt.ac.th*

ABSTRACT

The phosphate-aluminum-potassium-gadolinium glasses doped with Er₂O₃ were synthesized by the melt quenching technique. The density (ρ) has been measured using the Archimedes principle, and the molar volume (V_m) has also been estimated. The structural characterization of erbium-doped phosphate glass using FTIR spectra The optical absorption and fluorescence spectra were used to analyze the spectroscopic properties. The McCumber theory has been adopted in predicting the emission cross-section (σ_e) of $^4I_{13/2} \rightarrow ^4I_{15/2}$ transition from the absorption cross-section (σ_a) $^4I_{15/2} \rightarrow ^4I_{13/2}$ transition of Er³⁺ ions. The values of PAKGdEr1.5 stimulated absorption cross-section and emission cross-section are 1.128×10^{-20} cm² and 1.437×10^{-20} cm², respectively. The X-ray absorption near the edge structure of ErLIII-edge was investigated, and the absorption peak shown at ~8.362 keV confirmed the presence of Er³⁺ [1].

REFERENCES

1. Klug et al., Rev. Sci. Instrum. 86, 113901 (2015); <https://doi.org/10.1063/1.4934807>.

Structural correlation to optical properties of Er³⁺ ion doped alkali boro-phosphate glasses using synchrotron technique

N. Kiwsakunkran^{1,2}, N. Chanthima^{1,2,*}, P. Kidkhunthod³,
H. J. Kim⁴, S. Kothan⁵, J. Kaewkhao^{1,2}

¹Physics Program, Faculty of Science and Technology, Nakhon Pathom Rajabhat University, Nakhon Pathom 73000, Thailand

²Center of Excellence in Glass Technology and Materials science (CEGM), Nakhon Pathom Rajabhat University, Nakhon Pathom 73000, Thailand

³Synchrotron Light Research Institute, Nakhon Ratchasima 30000, Thailand

⁴Department of Physics, Kyungpook National University, Daegu, 41566, Republic of Korea

⁵Center of Radiation Research and Medical Imaging, Department of Radiologic Technology, Faculty of Associated Medical Sciences, Chiang Mai University, Chiang Mai, 50200, Thailand

**Email: natthakridta@webmail.npru.ac.th*

ABSTRACT

The different alkali oxide (lithium/sodium/potassium) boro-phosphate glasses activated with Er³⁺ ion were synthesised by the melt quenching technique. The surrounding environment for the Er³⁺ ion in these glasses was investigated by X-ray absorption spectroscopy (XAS). The Er LIII-edge white line XANES spectra of the glasses demonstrate the pronounced absorption peak at 8363 eV and show a +3 oxidation state, also confirming the presence of Er³⁺ in glasses. EXAFS analysis showed that the inter-atomic distance and Debye-Waller factor between Er-O for first shell value of lithium is larger than both of sodium and potassium glasses. This leads to in the lithium glass sample containing ability to more absorb and emit light. Judd-Ofelt (JO) parameters indicates that the potential for using as a lasing medium, which lithium glass exhibited the highest values of these parameters. In the present investigation, the results of EXAFS, absorption spectra, emission spectra, and JO analysis parameters are highly congruent.

Synchrotron Radiation Science in Industrial Materials

M. Ree¹

*Ceko Surface Technology Institute & Pohang Accelerator Laboratory
Republic of Korea
E-mail: ree@ceko.co.kr; ree@postech.edu; reemoonhor@gmail.com*

ABSTRACT

Synchrotron radiation science, as a powerful tool, has been strongly engaged in the research and development of advanced industrial materials. In this SLRI Users Meeting, three different material subjects investigated with 3rd and 4th synchrotron radiation sources will be presented.

Using 3rd-generation synchrotron radiation source, static X-ray scattering measurements were performed on the magnetic nanoparticles being developed for biomedical applications; the scattering data were quantitatively analyzed and resulting morphology details were correlated to magnetic property performance. Real-time X-ray scatterings were further conducted on mechanical stress induced morphology deformation/destruction and void creation/growth. In addition, 4th-generation synchrotron source (X-ray free electron laser: XFEL) was utilized to understand melting dynamics of metal nanoparticles.

Synchrotron studies of Ag⁺ and Dy³⁺ ions in zinc lanthanum aluminum borate glasses synthesized using Novel Microwave melt-quenching technique

P. Mangthong^{1,2}, N. Srisittipokakun^{1,2}, R. Rajaramakrishna², J. Abhiram³,
W. Busayaporn⁴, S.Kothan⁵, J. Kaewkhao^{1,2},

¹Physics Program, Faculty of Science and Technology, Nakhon Pathom Rajabhat University, 73000, Thailand

²Center of Excellence in Glass Technology and Materials Science (CEGM), Nakhon Pathom Rajabhat University, Nakhon Pathom 73000, Thailand

³Department of Post Graduate Studies and Research in Physics, The National College, Jayanagar, Bengaluru 560070, Karnataka, India

⁴Synchrotron Light Research Institute, Nakhon Ratchasima 30000, Thailand

⁵Center of Radiation Research and Medical Imaging, Department of Radiologic Technology, Faculty of Associated Medical Sciences, Chiang Mai University, Chiang Mai, 50200, Thailand

*Email: pmangthong@hotmail.com

ABSTRACT

A novel microwave heating technique is used in the present work to synthesize the glasses. In this work, the stoichiometry ratio of $(43-x) \text{ B}_2\text{O}_3 + 45\text{ZnO} + 5\text{La}_2\text{O}_3 + 5\text{Al}_2\text{O}_3 + 0.5\text{SnO}_2 + 1.5\text{AgNO}_3 + x\text{Dy}_2\text{O}_3$ was exposed to microwave energy, with 800-watt power, holding time was 26 min to synthesize by novel melting in the microwave and quenched suddenly. The study focused on borosilicate glasses such as physical, optical, structure, and luminescent characteristics. The prepared glasses were subjected to evaluate density, molar volume, and refractive index. The optical absorption spectra of glasses were measured in the range of 200 - 2000 nm. The surface plasmon resonance of AgNPs peaks resonates with the radiative transitions of Dy₂O₃ ions at 426 nm. The emission spectra in the visible region showed three peaks in the range of 450 - 700 nm, and the excitation spectra of developed glass samples in the range of 200 - 500 nm, the most intense peak was observed at 351 nm. The creation of consistent circular shape nanoparticles and interplanar distance was confirmed by SAED and HRTEM respectively. XANES measurement reveals the oxidation status of Dy³⁺ ions and Ag⁺ ions. The coordination chemistry of Dy₂O₃ in the present glass was analyzed and discussed their Dy-O bond length based on the first shell fitting using EXAFS.

REFERENCES

- [1] N.P.N. Sio, E. Ternary, (2018) 15–17.
- [2] J. Miranda de Carvalho, C.C.S. Pedroso, M.S. de N. Saula, M.C.F.C. Felinto, H.F. de Brito, *Molecules*. 26 (2021).
- [3] Y.S.M. Alajerami, K.M. Abushab, S.I. Alagha, M.H.A. Mhareb, A. Saidu, F.S. Kodeh, K. Ramadan, *Int. J. Mod. Phys. B*. 31 (2017) 2–5.
- [4] R. Vijayakumar, R. Nagaraj, P. Suthanthirakumar, P. Karthikeyan, K. Marimuthu, *Spectrochim. Acta - Part A Mol. Biomol. Spectrosc.* 204 (2018) 537–547.
- [5] P. Narwal, M.S. Dahiya, A. Yadav, A. Hooda, A. Agarwal, S. Khata, Elsevier Ltd and Techna Group S.r.l., 2017.

Synthesis and characterization of Gd₂MoB₂O₉: CeF₃ phosphors doped ZnO: BaO: B₂O₃ glasses by microwave sintering for scintillation materials

W. Wongwan^{1,2*}, P. Yasaka^{1,2}, K. Boonin^{1,2}, H.J. Kim³, P. Kidkhunthod⁴
and J. Kaewkhao^{1,2}

¹Center of Excellence in Glass Technology and Materials Science (CEGM), Nakhon Pathom Rajabhat University, Nakhon Pathom 73000, Thailand

²Physics Program, Faculty of Science and Technology, Nakhon Pathom Rajabhat University, 73000, Thailand

³Department of Physics, Kyungpook National University, Daegu, 41566, Republic of Korea

⁴Synchrotron Light Research Institute, Nakhon Ratchasima, 30000, Thailand

Email: Winutwongwan@gmail.com

ABSTRACT

The aim of this present work is to investigate the physical, optical, structural, photoluminescence, and X-ray luminescence properties of Gd_{1.5}MoB₂O₉: 0.5CeF₃ doped 10ZnO:35BaO:55B₂O₃ glass with a weight ratio of 1:9 by the heating with microwave sintering method at the time for sintering varied from 5 min to 10 min. The structural studies using XRD and XANES analysis. An X-ray diffraction analysis (XRD) was used to investigate the samples' structure by a Shimadzu XRD-6100 diffractometer. XANES spectra of Ce-LIII edge for samples shows peaks at ~ 5728 eV confirming the presence of Ce³⁺ and Ce⁴⁺. Absorption spectra were recorded by using UV-VIS-NIR spectrophotometer (Shimadzu, 3600). The photoluminescence of samples shows the overlapping peaks between excitation and emission peaks in the range of 300 nm – 450 nm by monitoring at room temperature with a spectrofluorophotometer (Cary-Eclipse). These emissions correspond to the 5d – 4f transitions of Ce³⁺ ion. The x-ray-induced optical luminescence spectra showed a strong emission peak at 411 nm. The sample with the highest intensity is as efficient as 35.47% compared with bismuth germanium oxide (BGO) crystal. The results obtained in the present work demonstrate that the present samples could be a potential candidate for use in scintillator applications.

REFERENCES

1. W. Wongwan, et.al., Scintillation and photoluminescence investigations of Gd₂MoB₂O₉: CeF₃ phosphors, 2022. Radiation Physics and Chemistry, 199.
2. Som, S., Sharma, S.K., Lochab, S.P., 2013. Ion induced modification of bandgap and CIE parameters in Y₂O₃:Dy³⁺ phosphor. Ceram. Int. 39 (7), 7693–7701.
3. Kaewkhao, J., Wantana, N., Kaewjaeng, S., Kothan, S., Kim, H.J., 2016. Luminescence characteristics of Dy³⁺ doped Gd₂O₃-CaO-SiO₂-B₂O₃ scintillating glasses. J. Rare Earths 34 (6), 583–589.
4. Rajaramakrishna, R., Kaewjaeng, S., Kaewkhao, J., Kothan, S., 2020. Investigation of XANES study and energy transport phenomenon of Gd³⁺ to Ce³⁺ in CaO-SiO₂-B₂O₃ glasses. Opt. Mater. 102, 109826
5. Wu, J., Yan, B., 2010. Room-temperature solid-state reaction behavior, hydrothermal crystallization and physical characterization of NaRE(MoO₄)₂ and Na₅Lu₂(MoO₄)₂ compounds. J. Am. Ceram. Soc. 93, 2188-2194.
6. Zaman, F., Kaewkhao, J., Rooh, G., Srisittipokakun, N., Kim, H.J., 2016. Optical and luminescence properties of Li₂O-Gd₂O₃-MO-B₂O₃-Sm₂O₃ (MO=Bi₂O₃, BaO) glasses. J. Alloys Compd. 676, 275-285.
7. Zhang, X., Seo, H.J., 2011. Luminescence properties of novel Sm³⁺, Dy³⁺ doped LaMoBO₆ phosphors. J. Alloys Compd. 509 (5)
8. Janani, K., Ramasubramanian, S., Thangavel, R., Thiyagarajan, P., 2019. Effect of gadolinium concentration on the luminescence of LiYF₄:Yb³⁺/Er³⁺ phosphor. J. Solid State Sciences 91, 199.

9. Zhang, X., Qiao, X., Seo, H.J., 2010. Redemission, LaMoBO6:Eu³⁺ phosphor for near-UV whitelight-emitting diodes. J. Electrochem. Soc. 157, 267–269.
10. Enneffati, Marwa, Maaloul, Nadia Khadija, Louati, Bassem, Guidara, Kamel, Khirouni, Kamel, 2017. Synthesis, vibrational and UV-visible studies of sodium cadmium orthophosphate. Opt. Quant. Electron. 49 (10), 331.

The investigation of Cu species transformation during the reduction of K⁺ doped copper phyllosilicate by the *in-situ* TR-XANES

W. Prasanseang¹, Y. Poo-arporn², K. Choojun^{1,3} and T. Sooknoi^{1,3}

¹Department of Chemistry, School of Science, King Mongkut's Institute of Technology Ladkrabang, Chalongkrung Road, Ladkrabang, Bangkok, 10520, Thailand

²Synchrotron Light Research Institute (Public Organization), 111 University Avenue, Muang District, Nakhon Ratchasima, 30000, Thailand

³Catalytic Chemistry Research Unit, School of Science, King Mongkut's Institute of Technology Ladkrabang, Chalongkrung Road, Ladkrabang, Bangkok, 10520, Thailand
Email: 61605010@kmitl.ac.th

ABSTRACT

Copper phyllosilicate (CuPS) is a promising catalyst precursor since they could provide highly dispersed copper (Cu⁰) with partially reduced copper (Cu⁺) species after reduction due to a strong interaction with silica support [1,2]. In addition, the Brønsted acid sites (BAS) form surface silanol could be formed at the interface of the Cu⁰. This could lead to a lower fatty alcohol selectivity from hydrogenation of FAMES [3]. Therefore, doping with alkali metal would be a promising method to reduce the BAS on CuPS [4]. In this study, the K⁺ were impregnated over calcined (K-CuPS) and reduced (K-rCuPS) CuPS for comparison. The transformation of Cu species during reduction were investigated by *in situ* TR-XANES experiments at BL2.2: TRXAS. The samples were firstly *in situ* calcined in 20%O₂/N₂ from RT to 400 °C for 2 h. After cooldown, the sample were reduced under 10%H₂/N₂ from RT to 250 °C and hold for 2 h. The Cu K-edge spectra were collected during reduction every 10 °C. In order to evaluate the Cu species during the experiments, the linear combination fitting (LCF) were performed using Athena Software. The Cu foil (8979.1 eV), Cu₂O (8980.5 eV) CuO (Cu²⁺ (Sq), 8990.2 eV) and CuSO₄ (Cu²⁺ (O_h), 8992.3 eV) were used standards for the fitting. The result shown that the all samples contained the mixing Cu²⁺ (O_h) and Cu²⁺ (Sq) species before reduction. However, the K-rCuPS provide highest Cu²⁺ (Sq) (~70%). This could indicate the re-oxidized of Cu metallic during the impregnation of K⁺. In addition, the added K⁺ could act as fluxing agent facilitate the reduction of Cu²⁺ to Cu⁰. Furthermore, after reduction at 250 °C for 2 h the K⁺ doped CuPS catalyst could maintain the Cu⁺ species in the order of CuPS (10.1%) > K-CuPS (11.5%) > K-rCuPS (14.1%), respectively.

REFERENCES

1. Chen, L. F., Guo, P. J., Qiao, M. H., Yan, S. R., Li, H. X., Shen, W., ... & Fan, K. N. (2008). Cu/SiO₂ catalysts prepared by the ammonia-evaporation method: Texture, structure, and catalytic performance in hydrogenation of dimethyl oxalate to ethylene glycol. *Journal of Catalysis*, 257(1), 172-180.
2. Jiang, J. W., Tu, C. C., Chen, C. H., & Lin, Y. C. (2018). Highly Selective Silica-supported Copper Catalysts Derived from Copper Phyllosilicates in the Hydrogenation of Adipic Acid to 1, 6-hexanediol. *ChemCatChem*, 10(23), 5449-5458.
3. Prasanseang, W., Choojun, K., Poo-arporn, Y., Huang, A. L., Lin, Y. C., & Sooknoi, T. (2022). Linear long-chain α -olefins from hydrodeoxygenation of methyl palmitate over copper phyllosilicate catalysts. *Applied Catalysis A: General*, 635, 118555.
4. Hu, D., Hu, H., Zhou, H., Li, G., Chen, C., Zhang, J., ... & Wang, L. (2018). The effect of potassium on Cu/Al₂O₃ catalysts for the hydrogenation of 5-hydroxymethylfurfural to 2, 5-bis (hydroxymethyl) furan in a fixed-bed reactor. *Catalysis Science & Technology*, 8(23), 6091-6099.

Tuning Surface Energy to Enhance MoS₂ Nanosheets Production via Liquid Phase Exfoliation: Understanding of Electrochemical Adsorption of Cesium Chloride

P. Chavalekvirat¹, P. Nakkiew¹, T. Kunaneksin¹, W. Hirunpinvopas²,
W. Busavapron³, and P. Iamprasertkun^{1,*}

¹*School of Bio-Chemical Engineering and Technology, Sirindhorn International Institute of Technology, Thammasat University, Pathum Thani 12120, Thailand*

²*Department of Chemistry and Centre of Excellence for Innovation in Chemistry, Faculty of Science, Kasetsart University, Bangkok 10900, Thailand.*

³*Synchrotron Light Research Institute (Public Organization), 111 University Avenue, Muang, Nakhon Ratchasima, 30000, Thailand*
Email: pawin@siit.tu.ac.th

ABSTRACT

Environmental pollution caused by radionuclides like Cs-137 and Cs-134 has increased global attention towards public health. Electrochemical adsorption has emerged as a feasible, rapid, and scalable method to treat contaminated water sources. However, graphene and its derivatives have limitations in ion adsorption via physisorption, forming a double layer that restricts the electrode's adsorption capacity. To address this, we propose the use of molybdenum disulfide (MoS₂) with its extensive intercalation galleries of MoS₂ nanosheets for cesium removal via electrochemical route. Liquid phase exfoliation with water and N-methyl-2-pyrrolidone (NMP) was then used to produce MoS₂ nanosheets in a scalable quantity (high-yield production). The formation of a mixed solvent possessing relatively equivalent surface energy for exfoliation enabled us to achieve remarkable exfoliation yield up to ca. 1.26 mg mL⁻¹, which is one of the highest yields reported to date (without surfactant being added), and to the best of our knowledge. The 35% v/v of water in NMP displayed a maximum yield, while maintaining the structure of the as exfoliated one. X-ray Absorption Spectroscopy (XAS) analysis verified that when the water content exceeded 66.7% v/v, the formation of MoO₃ occurred. Moreover, the insight into the cesium ions removal mechanistic through the electrochemical route was demonstrated. By analyzing the MoS₂ material using X-ray Photoelectron Spectroscopy (XPS) after 100 cycles in the presence of CsCl, it was observed that the elimination of Cs⁺ ions occurs primarily through electrochemical intercalation rather than adsorption. This work aids the understanding of cesium intercalation coupled with a mass-scale production method, which should lead to more efficient and cost-effective removal of radionuclides from contaminated water sources, opening new research avenues in materials and environmental science.

Utilizing Synchrotron Radiation for Characterizations of the p-Cu₂O and n-g-C₃N₄ Semiconductors for Tribovoltaic Nanogenerator Development

S. Worathat¹, S. Sriphan^{1,2}, P. Pakawanit³, N. Chanlek³
and N. Vittayakorn^{1,4}

¹*Advanced Material Research Unit, School of Science, King Mongkut's Institute of Technology Ladkrabang, Bangkok, 10520, Thailand*

²*Faculty of Science, Energy and Environment, King Mongkut's University of Technology North Bangkok, Bangkok, 10800, Thailand*

³*Synchrotron Light Research Institute, 111 University Avenue, Muang District, Nakhon Ratchasima, 30000 Thailand*

⁴*Department of Chemistry, School of Science, King Mongkut's Institute of Technology Ladkrabang, Bangkok, 10520, Thailand*
Email: saichon.s@sciee.kmutnb.ac.th

ABSTRACT

The tribovoltaic nanogenerator (TVNG) was recently developed to solve the operating issue of the triboelectric nanogenerator (TENG). The TVNG exhibits the prominent properties of direct current (DC) output generation and a high rate of charge transfer when compared with a traditional TENG [1]. The tribovoltaic effect is achieved by rubbing a metal/semiconductor on another semiconductor. The frictional energy released by the forming atomic bonds excites nonequilibrium carriers, which are directionally separated to form a current under the built-in electric field. Because of the recent development, urgent investigations of physical mechanisms and structural design are required. Additionally, seeking and expanding characterizations of novel tribovoltaic materials are essential for TVNG development. In this work, we presented the characterizations of new tribovoltaic materials, *i.e.*, p-Cu₂O and n-g-C₃N₄, using synchrotron radiation techniques including X-ray Photoelectron spectroscopy (XPS) and X-ray Tomographic Microscopy (XTM). Progress was efficiently used to gain insight into the materials in terms of phase structure and morphology. Moreover, the output performances of the proposed TVNGs based on the p-Cu₂O/n-g-C₃N₄ heterojunction in various device structures were introduced.

REFERENCES

1. Sriphan, S. and N. Vittayakorn, *Tribovoltaic effect: Fundamental working mechanism and emerging applications*. *Materials Today Nano*, 2023. 22: p. 100318.

UV-C sensors based on beta gallium oxide

S. Thongkaew¹, A. Rattanachata², H. Nakajima², W. Meevasana³ and
S. Ratanaphan^{1,4}

¹ Department of Tool and Materials Engineering, Faculty of Engineering, King Mongkut's University of Technology Thonburi, Bangkok 10140, Thailand

² Synchrotron Light Research Institute, Nakhon Ratchasima, 30000, Thailand

³ School of Physics, Suranaree University of Technology, Nakhon Ratchasima, 30000 Thailand

⁴ Center of Excellence in Theoretical and Computational Science Center (TaCS-CoE), Faculty of Science, King Mongkut's University of Technology Thonburi, 126 Pracha Uthit Rd, Thung Khru, Bangkok 10140, Thailand
Email: supitchaya.thongkaew@kmutt.ac.th

ABSTRACT

Long exposure of UV-C (280 nm) can cause skin cancers due to its high photon energy (4.4 eV). Because of the human-induced climate change, "low-ozone events" and high UV index rating are frequently observed in Thailand, leading to the propensities of the cancers in the future. However, UV-C sensors are significantly more expensive compared with infrared or visible sensors, indicating the need for the low cost of UV-C sensors. Considering that the photon energy of UV-C is closed to the bandgap energy of Beta-Gallium Oxide (β -Ga₂O₃, ~ 4.5 to 4.9 eV), it might be possible to use the β -Ga₂O₃ as an active material for UV-C sensors. Based on our recent study published in *Applied Physics Letters* 2021 [1], it was demonstrated that the dynamic changes of electrical conductance in the SrTiO₃ single crystals significantly correlated to the relative change of ultraviolet-induced oxygen vacancies measured by ultraviolet photoelectron spectroscopy (UPS) at beamline 3.2a synchrotron light research institute (Thailand). Therefore, it is believed that similar phenomenon could also be observed in the β -Ga₂O₃ single crystal irradiated by the UV-C. In this study, the dynamic changes of electrical conductance stimulated by the UV-C irradiation in the β -Ga₂O₃ single crystal are measured and compared with the relative change of ultraviolet-induced oxygen vacancies. The UV-C sensors show high responsibility and detectivity of 1 A/W and 1 x 10¹² Jones, respectively, indicating an interplay of the UV-C induced oxygen vacancies and its electrical conductance. The high responsibility and detectivity obtained from the β -Ga₂O₃ single crystal pave a new route for the low cost fabrication of UV-C sensors.

REFERENCES

1. M. Sriondee *et al.*, "Ultraviolet-induced oxygen vacancy in SrTiO₃ polycrystalline," *Appl. Phys. Lett.*, vol. 118, no. 22, p. 221602, Jun. 2021, doi: 10.1063/5.0048137.

Woven Fabric-based Triboelectric Nanogenerators: Effect of Weaving pattern and Multilayer Structure Design on the Electrical Output

P. Krailadsirattana¹, N. Kerdsoonthorn¹, A. Nikomkhet¹, S.Pongampai²,
S. Plaipichit³, P. Pakawanit⁴, N. Vittayakorn⁵, T. Charoonsuk^{1*}

¹Department of Materials Science, Faculty of Science, Srinakharinwirot University,
Sukhumvit 23, Watthana, Bangkok 10110, Thailand

²Department of Physics, Faculty of Science, King Mongkut's University of Technology
Thonburi, Bangkok 10140, Thailand

³Department of Physics, Faculty of Science, Srinakharinwirot University, Sukhumvit 23,
Watthana, Bangkok 10110, Thailand

⁴Synchrotron Research and Applications Division, Synchrotron Light Research Institute, 111
University Avenue, Muang District, Nakhon Ratchasima, 30000, Thailand

⁵Advanced Materials Research Unit, School of Science, King Mongkut's Institute of
Technology Ladkrabang, Bangkok 10520, Thailand

*Email: thitiratc@g.swu.ac.th

ABSTRACT

Nowadays, the triboelectric nanogenerator (TENG) [1] that can convert mechanical energy into electrical energy based on triboelectricification and electrostatic induction generated has attracted considerable interest as a powerful power source for the electronic textiles (E-textiles) has received great interest in development. This research focused in the development of textile-TENG (T-TENG) using woven fabric as the main contact material and design the multi-layer structure to improve its efficiency. The type of intermediate layer which consists of ball fibers, synthetic fibers, microgel fibers, and kapok fibers related to electrical output signal is studied. The internal functional group of fiber was confirmed by infrared spectroscopy (IR) techniques. According to the important role of microstructure inside fabric, the Synchrotron Radiation X-ray Tomographic Microscopy (SR-XTM) technique was selected to examine differences in the internal structure of each fiber type. It was found that even through having similar chemical structure, the ball fibers 3D morphology characteristics are significant difference. It results in showing high performance. The T-TENG device with ball fibers provide the highest electrical output of ~3.34 V for output voltage (V_{oc}) and ~49.82 μA for output current (I_{sc}). This work can therefore confirm the possibility way of developing multilayer structure fabric based TENG in industrial E-textiles for future.

REFERENCES

1. G. Zhu, B. Peng, J. Chen, Q. Jing, and Z. Lin Wang., *Nano Energy*, 14,126-138 (2015).



**THAI
SYNCHROTRON**
NATIONAL LAB

Contact us:



User Service Section

Synchrotron Light Research Institute (Public Organization)



66 44 217 040 Ext. 1602 – 1605



userservice@slri.or.th